

Final Report
for
MICROWAVE RADIOMETER DESIGN AND DEVELOPMENT

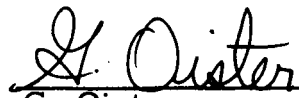
Volume I of 2 Volumes

15 November 1967

Contract No. NAS 5-9680

Goddard Space Flight Center
Contracting Officer: R. L. Krenning
Program Officer: C. Catoe


C. U. Falco
Advanced Microwave
Systems Division


G. Oister
Program Manager

Prepared by
Aerojet-General Corporation
Space Division
9200 East Flair Drive
El Monte, California

for
Goddard Space Flight Center
Greenbelt, Maryland

SUMMARY AND CONCLUSIONS

The Nimbus Radiometer was designed to be a precisely calibrated instrument for recording and accurately displaying absolute meteorological radiometric temperatures of a wide variety of atmospheric and terrain conditions. Celestial objects such as sky and sun temperatures are used as calibration references.

The objective planned and achieved was to design and deliver a meteorological radiometric instrument with absolute temperature measurement capability.

A high degree of precision and repeatability in recording and display of these objects was also required. In order to accomplish these objectives, an extremely precise set of test and calibration procedures, together with necessary equipment was planned.

This set of tests and procedures consisted of individual component insertion loss measurements and overall system calibration. Calibrated cryogenic loads and accurately measured hot loads were fabricated and used for these tests. These loads consisted of secondary standards which were referred to primary standards at N. B. S. These references provide measurements at least 100 times more accurate than required system specifications.

In addition to precision bench tests, insertion loss, beam efficiency and absolute calibration tests were performed in the radiometric mode against atmospheric and galactic references at the JPL Table Mountain test site. The instrument, as delivered, is very satisfactory in meeting these objectives. A small negative offset appeared in aircraft model only. The detailed results of calibration and tests may be seen in Appendixes XX through XXIV.

The instrument has, in most specification categories, met or exceeded the original requirements as shown in Table 2-1, page 2. The phased array, electrically scanned waveguide antenna performs satisfactorily and meets most of the original design requirements. The solid-state radiometer, including the superheterodyne receiver with its solid-state local oscillator and varactor

- multiplier operating at 19.35 GHz, has proven to be reliable. Also, the signal processing digital and display portions of the system perform as required.

The radiometer was accepted after the second power-on flight by C. Catoe Technical Officer for GSFC on May 6, 1967.

The technical and contractual history of the Nimbus Meteorological Radiometer program, from its inception to its conclusion, is presented herein. In addition to the analysis and conclusions, a photographic record of the equipment and special components is included in Volume I. The scope of work encompassed:

- Two models (satellite model replaced with aircraft model, in accordance with revision of scope of work, dated April 1966)
- Two flight tests
- Data acquisition system
- Computer programming
- Test sets
- Recording and display system

On April 24, 1967, the aircraft model microwave radiometer and data acquisition system was delivered to Ames Research Center, Moffett Field, for installation aboard the 990 Convair Aircraft. Installation and checkout was completed by May 3, 1967. The first power on flight was May 5, 1967. Maps were made by use of the facsimile recorder and data was recorded using the digital tape recorder. The equipment appeared to perform successfully, however, white traces occurred across the width of the map. Checkout of the equipment revealed no malfunction. On May 6, 1967, the second power-on flight was made and the white traces were determined to be RFI on the one pulse per second line coming from the aircraft timing generator. By disconnecting the one pulse per second line the white traces disappeared, resulting in better quality maps. No serious difficulties were present during these flights. Some operator proficiency was required to adjust the contrast and white levels of the facsimile machine to the proper levels. This proficiency was quickly acquired by the end of the second flight and operation became routine.

A complete and precise absolute-temperature calibration was performed prior to installation on the aircraft, and the results were satisfactory.

Subsequent analysis of the data indicated that low temperature calibration is almost perfect, however, at the high temperature end of the dynamic range, a slight offset was noted which will be corrected in future installations by means of another waveguide switch installed ahead of the Dicke switch.

The tests at Ames proved successful, as shown by the facsimile maps which were processed at that time. It was concluded that, because of the extreme variations in radiometric temperature differentials, an automatic contrast control could be used on the facsimile system. For example, one target area may have a radiometric temperature differential of 290° to 310° Kelvin, while another target area may have a temperature differential of 100° to 330° Kelvin. Compression or expansion in the dynamic range could be accomplished within the data processing portion of the system.

CONTENTS

	<u>Page</u>
SECTION 1 - INTRODUCTION	1
SECTION 2 - RADIOMETER	2
2.1 General	2
2.2 Antenna	14
2.3 Dicke Switches and Hot and Cold Loads	20
2.4 Receiver	23
2.5 Bench Test Equipment	30
2.6 Table Mountain Tests	35
2.7 Aircraft Model	40
SECTION 3 - NIMBUS RADIOMETER TEST SET	44
3.1 Microwave Source	44
3.2 Telemetry Interface Circuitry	44
SECTION 4 - DATA ACQUISITION AND DISPLAY SYSTEM	56
SECTION 5 - CALIBRATION	61
Appendix I NIMBUS Radiometer Antenna Patterns	I-1
Appendix II Ferrite Circulator-Switches	II-1
Appendix III Position of Horizontally-Polarized Grating Lobes	III-1
Appendix IV Effect of Waveguide Tolerances on Phase Front of Ported-Array Elements	IV-1
Appendix V Review of Basic RF Preamplifier Gain Requirements for the NIMBUS Radiometer Receiver	V-1
Appendix VI Phase-Shifter Coil Requirement	VI-1
Appendix VII Beam Angle for 94 Percent Crossover	VII-1
Appendix VIII Phase Shifter and Drive Requirements	VIII-1
Appendix IX Suppression of a Cross-Polarized Field With a Ground Plane	IX-1
Appendix X Monte Carlo Analysis	X-1
Appendix XI Beam Positions for Scanning and Other Miscellaneous Topics	XI-1
Appendix XII Beam Efficiency of a Scanning Planar Array Antenna	XII-1
Appendix XIII Continuous One-Piece Waveguide Flange for the NIMBUS Antenna	XIII-1
Appendix XIV Phase Shifter Drive/Bias Coil; Fundamental Design	XIV-1

CONTENTS (Continued)

		<u>Page</u>
Appendix XV	An Electronically-Scanned K-Band Phased Array for Space-Borne Radiometric Applications	XV-1
Appendix XVI	Antenna Pattern Range for Space-General Corporation	XVI-1
Appendix XVII	NIMBUS Breadboard Linearity Measurements . . .	XVII-1
Appendix XVIII	The Measurement of ΔT	XVIII-1
Appendix XIX	Circuit Description of NIMBUS IF Amplifier, Post Detection, and Switch Driver Circuits	XIX-1
Appendix XX	Bench Calibration of Meteorological Satellite Radiometer.	XX-1
Appendix XXI	Measurement of NIMBUS Antenna Radiometric Efficiency	XXI-1
Appendix XXII	Preliminary NIMBUS Breadboard Test Procedure (Preliminary Testing)	XXII-1
Appendix XXIII	NIMBUS Radiometer Test Set - Telemetry Interface Circuitry	XXIII-1
Appendix XXIV	Evaluation of the Breadboard Microwave Meteorological Radiometer and Scanning Antenna	XXIV-1
Appendix XXV	Frequency Stability of Solid State Source	XXV-1
Appendix XXVI	Test Results of Solid State Source	XXVI-1
Appendix XXVII	NIMBUS Phase Shifter Design	XXVII-1
Appendix XXVIII	A Solid State Local Oscillator Source at 19.35 GHz	XXVIII-1
Appendix XXIX	Antenna Measurements	XXIX-1
Appendix XXX	Cryogenic Bench Test Set	XXX-1
Appendix XXXI	Relations for the Exact Calculation of Radiometric Temperatures of Cryogenic-Cooled Sources	XXXI-1

ILLUSTRATIONS

	<u>Page</u>
1 Breadboard System Block Diagram of NIMBUS Microwave Radiometer	4
2 Hot Load Versus Antenna Temperature	5
3 IF Bandwidth	5
4 Radiometer Framing Format	7
5 Aircraft Command Relay Module	8
6 Aircraft Beam Steering Computer	9
7 Aircraft/Breadboard Beam Steering Computer	10
8 Aircraft Model Coil Current Readout Module	11
9 Breadboard Radiometer and Phased Array	16
10 Aircraft Antenna	18
11 Timing and Control Counter, Schematic Diagram	21
12 Timing and Control Counter, Block Diagram	22
13 Balanced Mixer, Aircraft and Breadboard	24
14 Solid-State Local Oscillator, Aircraft and Breadboard	25
15 Solid-State Multiplier	26
16 Solid-State Source, Aircraft and Breadboard	27
17 Solid-State Source, 19.35 GHz, Aircraft and Breadboard	28
18 Bench Test Set Console	31
19 Cryogenic Equipment, Bench Test Set, Two Port	32
20 Cryogenic Bench Test Set, Two Port	33
21 Cryogenic Equipment, Aircraft Model, Single Port	34
22 Breadboard Radiometer and Phased Array Tests at Space-General	36
23 Field Test at Space-General Plant	37
24 Aircraft Model Antenna Test Boom (on Space-General Antenna Range)	38
25 Table Mountain Beam Efficiency Measurement	39
26 One Half of 4/4 Aircraft Module	41

ILLUSTRATIONS (Continued)

	<u>Page</u>
27 Aircraft Flight Recording and Digital to Analog System. . . .	42
28 Scan Converter, Data Acquisition System	43
29 Block Diagram of NIMBUS Radiometer Test Set	45
30 NIMBUS Radiometer Test Set "B", Rack Number 2	47
31 NIMBUS "D" VIP Digital "A" Interface	48
32 NIMBUS Radiometer Test Set "A" Binary-to-BCD Converter, Rack 1	50
33 NIMBUS Radiometer Test Set "C", Rack Number 2	53
34 NIMBUS Radiometer Test Set Input-Output Connectors . . .	55

Section 1

INTRODUCTION

Volume I of this report consists of a general description of the project and the radiometer, including theory and operation of the instrument. Illustrations, tables, calibration information and procedures are also contained in Volume I, although, this calibration information is in summary form only. Detailed calibration procedures are contained in the Calibration Handbook. Volume II contains details of analysis and solutions to various design problems, as well as, calibration techniques, including bench and field tests.

Two models of the NIMBUS meteorological radiometers were originally planned: One, a breadboard model to test the feasibility, and the second, a satellite model. However, during the program review meeting, the scope of work was changed so that the second model was to be used as an aircraft model instead of a satellite model, as originally planned.

This report describes the overall project, the system, subsystem, and components. The main portions of the complete system were planned as follows:

- Radiometer, consisting of four basic parts:
 - Antenna, with its beam switching system
 - Dicke switching, including calibration and control subsystem
 - Receiver, consisting of RF mixer, IF amplifier, AGC, and second detector
 - Signal processing subsystems
- Test sets, consisting of hot and cold load calibrating subsystem and test and control subsystem

Each of the main portions of the overall system is described in varying degrees of detail in the following sections of this report. Also, where it is deemed necessary, photographs of the equipment are included.

Section 2

RADIOMETER

2.1 GENERAL

As a result of changes in requirements, two similar but different radiometers were designed and fabricated under this contract. A breadboard radiometer was designed and fabricated to be used under static conditions, such as; laboratory measurements, field measurements, i. e., radiometers supported from Towers, looking straight up, etc. The second set of equipment was to be used on an aircraft where dynamic measurements were to be made. The table below indicates the difference in specifications for the two systems.

Table 2-1

COMPARISON OF SPECIFICATIONS

	<u>Original Specs</u>	<u>Breadboard</u>	<u>Aircraft</u>
Sensitivity (ΔT)	0.7°K	0.7°K 0.1°K	1.4°K (2 sec) 2.1°K (1 sec)
Absolute accuracy within 2°K			
Scan Modes	Linear Stepped Scan Fixed Beam Position	Linear Stepped Scan Selectable Beam Positions	Linear Stepped Scan Fixed Beam Positions
Scan Time	8 sec	8 sec	1 sec
Beam Eff.	92%	92%	92%
Beam Width	2.85°	2.85°	2.85°
Power	20 watts	20 watts	20 watts
Ant. Losses	1.3 dB	2.6 dB	1.75 dB
Data Acq. Sys.	None Paper Printout	None Paper Printout	Real time map Nixie Readout Digital Tape Recording
Scan	<u>+50°</u>	<u>+50°</u>	<u>+50°</u>
Dynamic Range	100°K to 300°K	100°K to 38°K	100°K to 38°K

The breadboard system block diagram is shown in Figure 1. (Numbers have been assigned to the individual blocks, to correspond with the following discussion.) A description of the theory and functional operation of the system is as follows.

Radiation, directly proportional to the temperature, emitted by a body, is received by the planar array antenna (Block 1). The radiation selected encompasses a band of 400 MHz centered around 19.35 GHz. From the output port of the antenna the energy is coupled to a ferrite switch (Block 2). This is an aperiodic switch and for the moment will be considered unenergized. The energy passes through this switch to a second ferrite switch (Block 3) which is switching at a 600 Hz periodic rate between ferrite switch number 1 and a hot reference load (Block 20). The output of the switch is connected to a microwave mixer (Block 4). The mixer then is connected to the hot reference load for 1/1200 of a second and to the antenna through ferrite switch number 1 for 1/1200 of a second. Thus, if a difference in temperature exists between the temperature seen by the antenna and the temperature of the hot load, a square wave of a 600 Hz periodic rate will appear at the mixer. (Figure 2). By measuring the difference which is the square wave amplitude, the temperature of the body as seen by the antenna can be determined.

The frequency of the energy at the mixer port is 19.35 GHz and is converted down to a band of energies 200 MHz wide centered at 130 MHz. The conversion is achieved by the superheterodyne method. Thus, the oscillator (Block 5) as shown in the block diagram (Figure 1) is tuned to 19.35 GHz. The LO supplies approximately 2 mW of power at a frequency of 19.35 GHz to the mixer in order to generate the difference frequency at the IF passband.

The LO is composed of a transistor oscillator whose output drives two 4 x 4 varactor diode multipliers. Adequate feedback and proper bias level allows for stability of 2 parts in 10^{-5} over the temperature range of -5°C to $+55^{\circ}\text{C}$. Power output and impedance match are relatively unaffected by temperature. NBDS TM No. 27 gives a detail description of the operational parameters for the solid state source.

The IF bandwidth is 200 MHz with a center frequency of 130 MHz. As shown in Figure 3 it can be seen that the bandwidth of the system is 400 MHz due

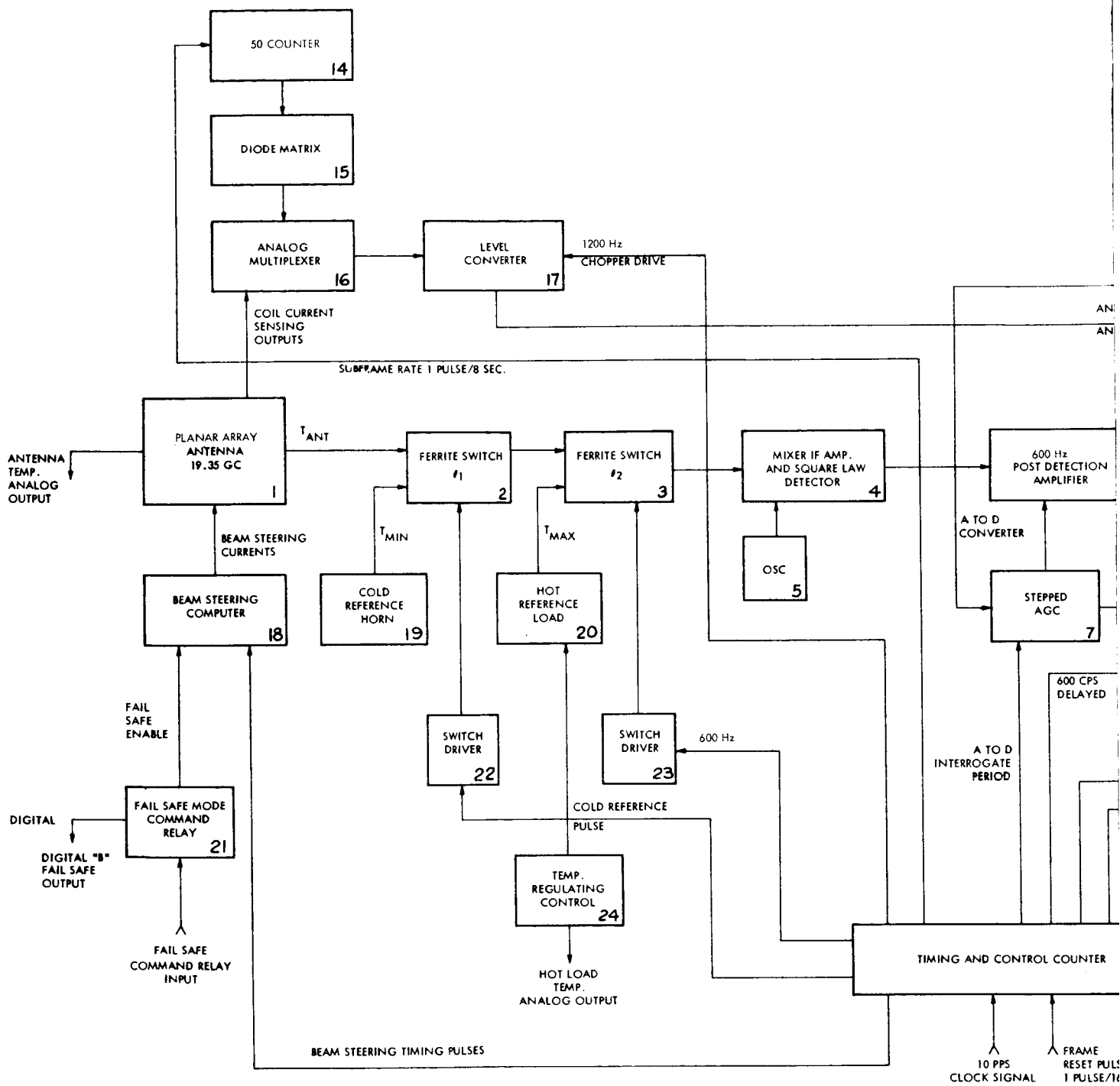


Figure 1. Breadboard System (NIMBUS Micro)

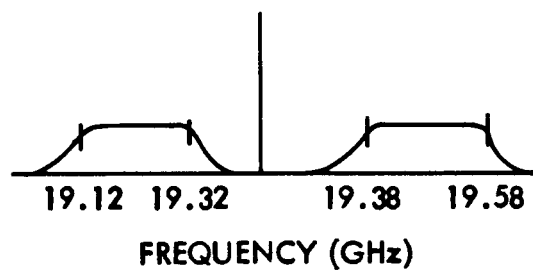
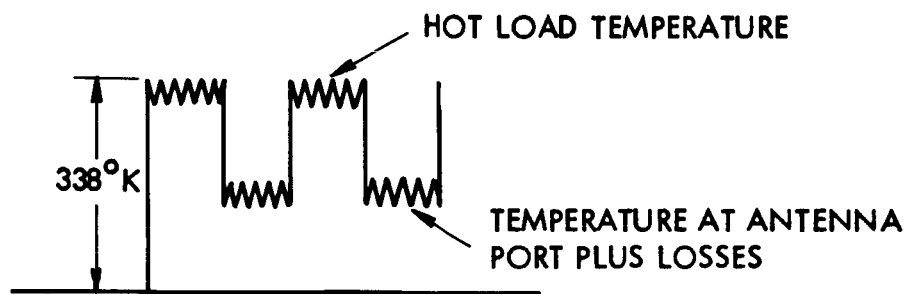


Figure 3. IF Bandwidth

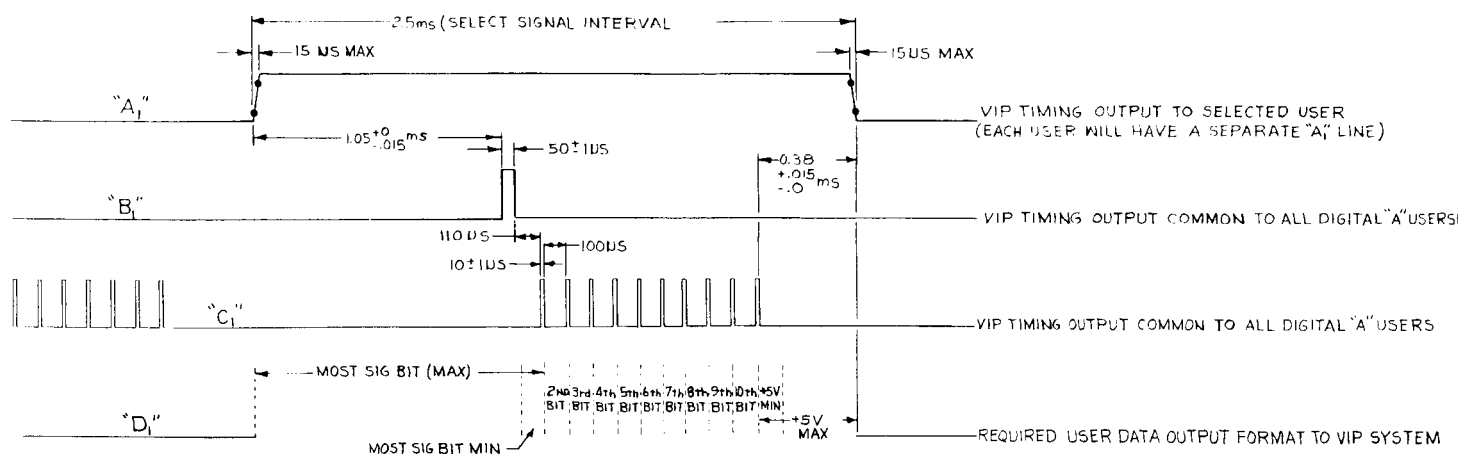
to the fold over of the image. The mixer is amplified by a broadband IF amplifier (Part of Block 4). The gain of this amplifier is chosen to sufficiently overcome noise in the 2nd detector. The output of IF amplifier is fed into the square law detector (Part of Block 4). The square law detector demodulates the square wave envelope created by the switching between the antenna and hot reference load. The output of the square law detector is a 600 Hz square wave. This signal is then full wave rectified by the 600 Hz synchronous detector (Block 8) whose output is a dc level proportional to the square wave modulation. This in turn is proportional to the temperature difference between the antenna brightness temperature and hot load reference temperature. The output of the 600 Hz synchronous detector (Block 8) is coupled to the analog multiplexer (Block 10). The analog multiplexer time-multiplexes the antenna brightness temperature with other parameters such as (1) antenna thermal temperature, (2) hottest spot in the module, (3) prime power supply voltage, (4) hot reference load thermal temperature, (5) one spare. The analog multiplexer time sequence is given by Figure 4.

The antenna current readout command relay (Block 28), on command, connects the analog multiplexer to the current sensing resistors in the antenna beam steering computer (Block 18). It also inhibits the stepped AGC, Block 7 and all other multiplexed parameters, and antenna brightness temperature outputs from the 600 Hz synchronous detector. In this mode the antenna current readout command relay connects coil 1 of the antenna phase shifter to the multiplexer for its 39 discrete currents then it steps to coil number 2 for its discrete currents and so forth for the 49 coils. In this manner the antenna coil currents can be measured for an indication of antenna operation.

Figures 5 through 8 show the equipment involved in these measurements.

The output of the multiplexer is connected to the integrate and dump (Block 11). This circuit integrates the antenna brightness temperature for 198.5 milliseconds. After that period of time the integrating filter is discharged for 1.5 milliseconds.

At this period of time all charge has been removed and the integrate and dump filter begins the recharging cycle for 198.5 milliseconds. After this period the charge is removed for 1.5 milliseconds. This process repeats at this periodic interval. The two-hundred milliseconds corresponds to the dwell time for an antenna beam position. The integrate and dump filter is used for two



REQUIRED OUTPUT CHARACTERISTICS

"A₁": AMPLITUDE 0[±]0.6 VOLTS OR +5[±]0.6 VOLTS, Z₀ = 5,000 ohms OR LESS

"B₁": AMPLITUDE 0[±]0.6 VOLTS OR +5[±]0.6 VOLTS, Z₀ = 600 ohms OR LESS, RISE & FALL TIME LESS THAN 1 μs

[USER LOAD IMPEDANCE: 20,000 ohms MIN.; CAPACITIVE LOAD 25 pf MAX.; TRANSFORMER COUPLING RECOMMENDED]

"C₁": AMPLITUDE 0[±]0.6 VOLTS OR +5[±]0.6 VOLTS, Z₀ = 600 ohms OR LESS, RISE & FALL TIME LESS THAN 1 μs

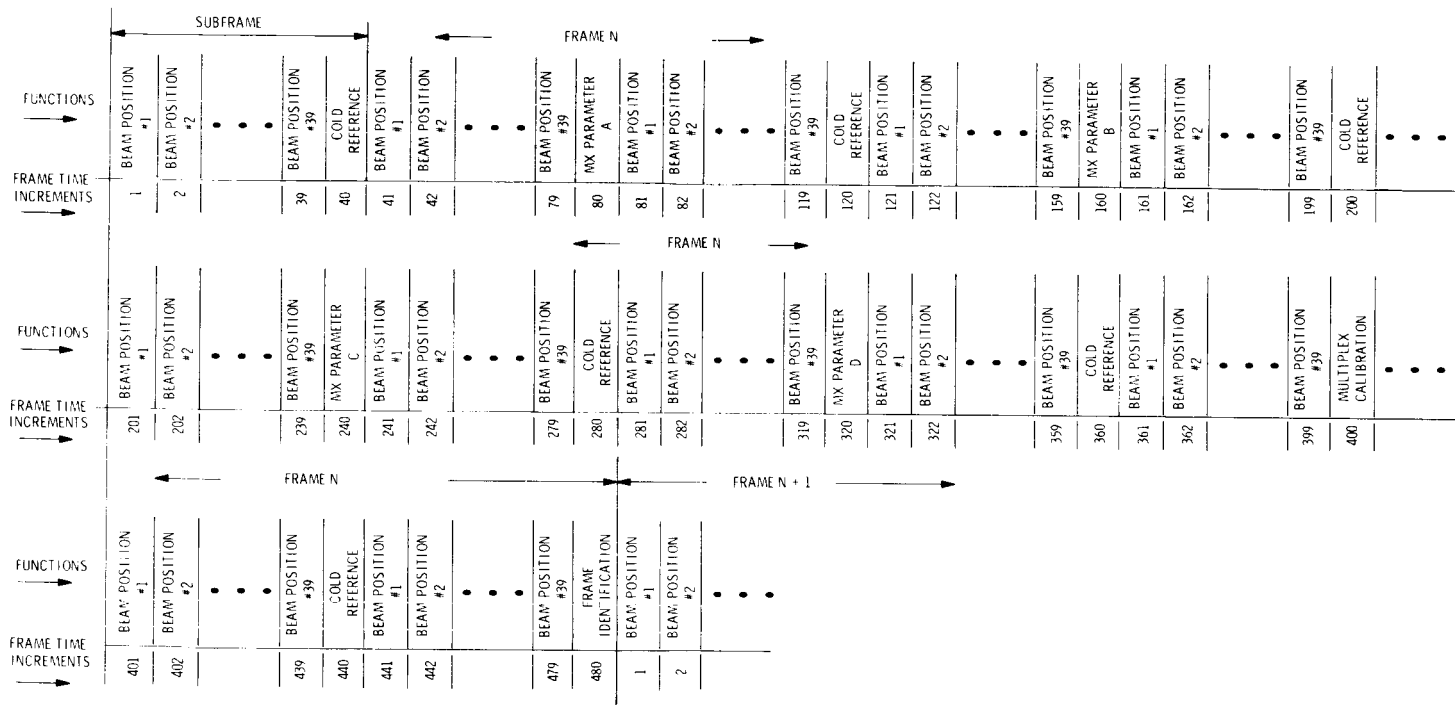
[USER LOAD IMPEDANCE: 20,000 ohms MIN.; CAPACITIVE LOAD 25 pf MAX.; TRANSFORMER COUPLING RECOMMENDED]

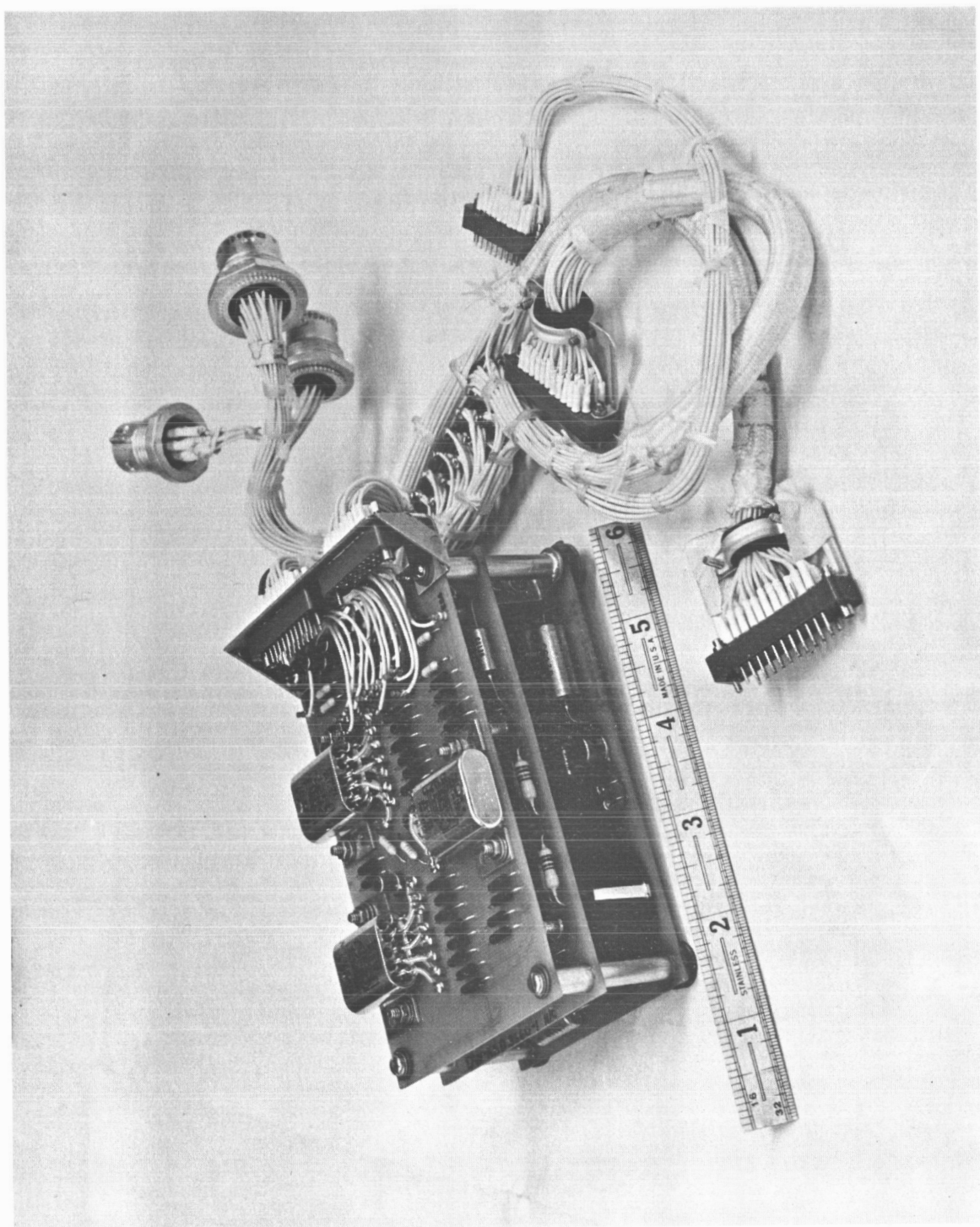
"D₁": AMPLITUDE 0[±]0.6 VOLTS FOR LOGICAL "0" AND +5[±]0.6 VOLTS FOR LOGICAL "1", RISE & FALL TIME LESS THAN 1 μs WITH EXPERIMENT POWER ON OR OFF, USERS "D₁", LOAD IMPEDANCE SHALL BE 1000 ohms OR LESS

Figure 4. Radiometer Framing

7-A

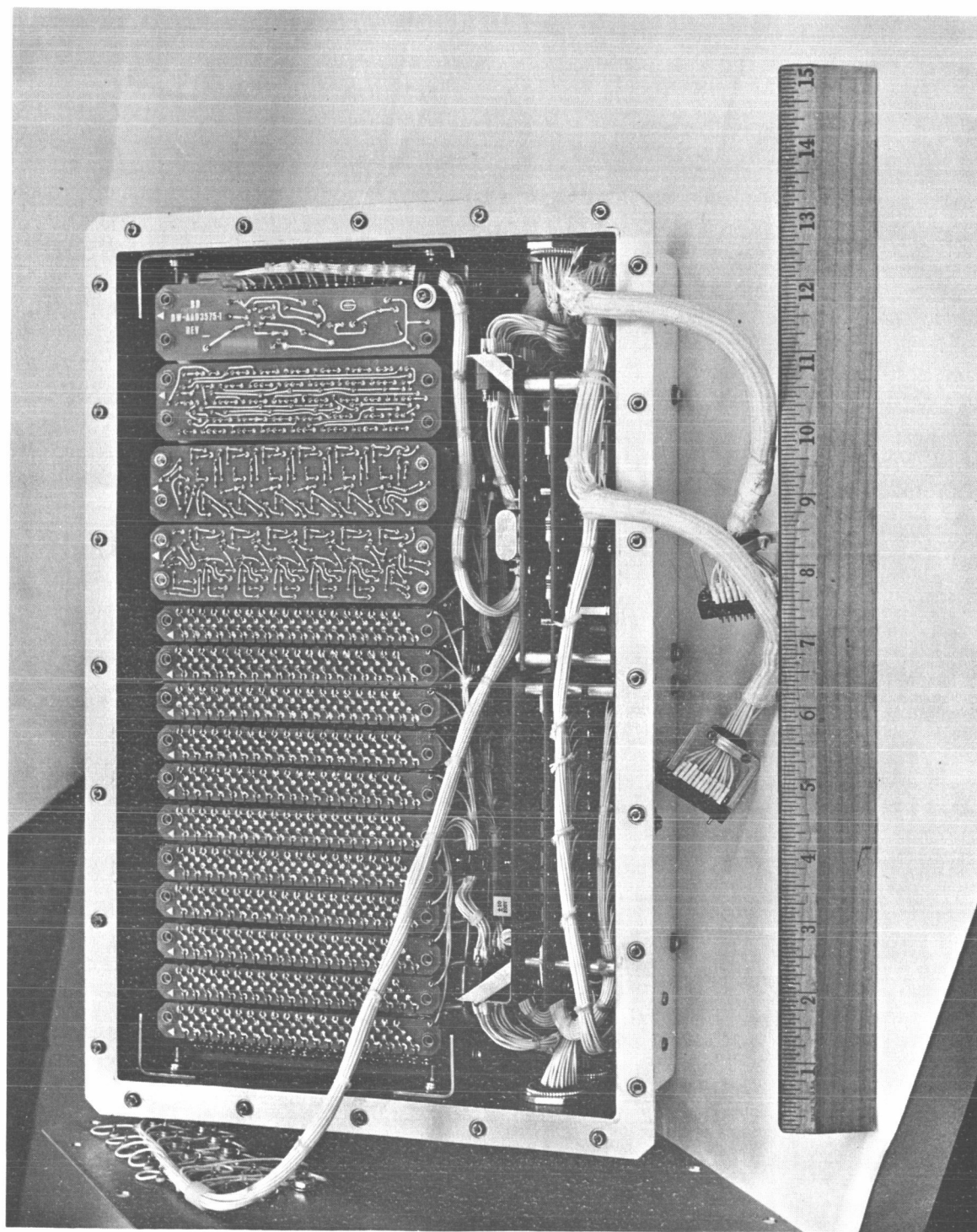
g Format





939/065

Figure 5. Aircraft Command Relay Module



939/063

Figure 6. Aircraft Beam Steering Computer

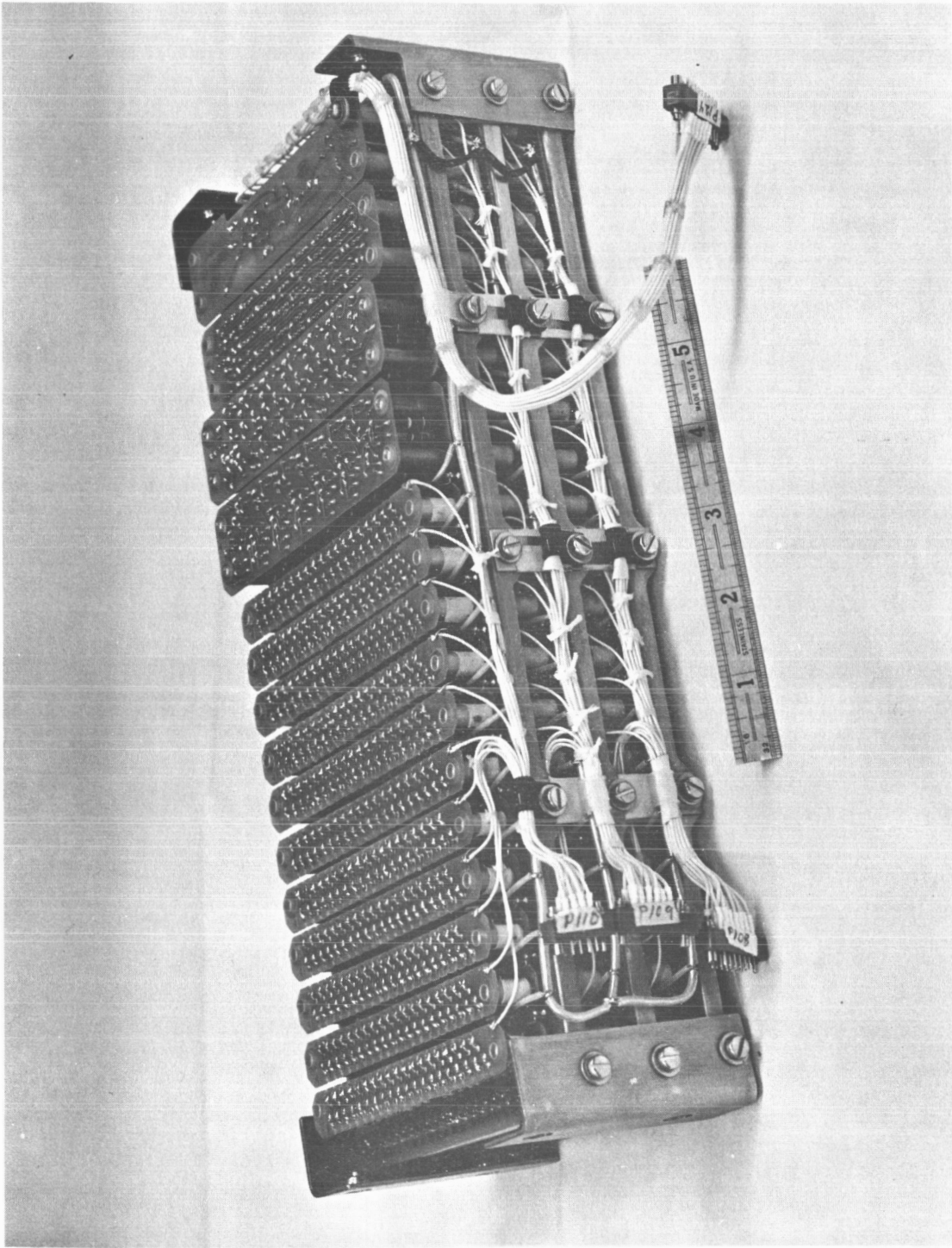


Figure 7. Aircraft/Breadboard Beam Steering Computer

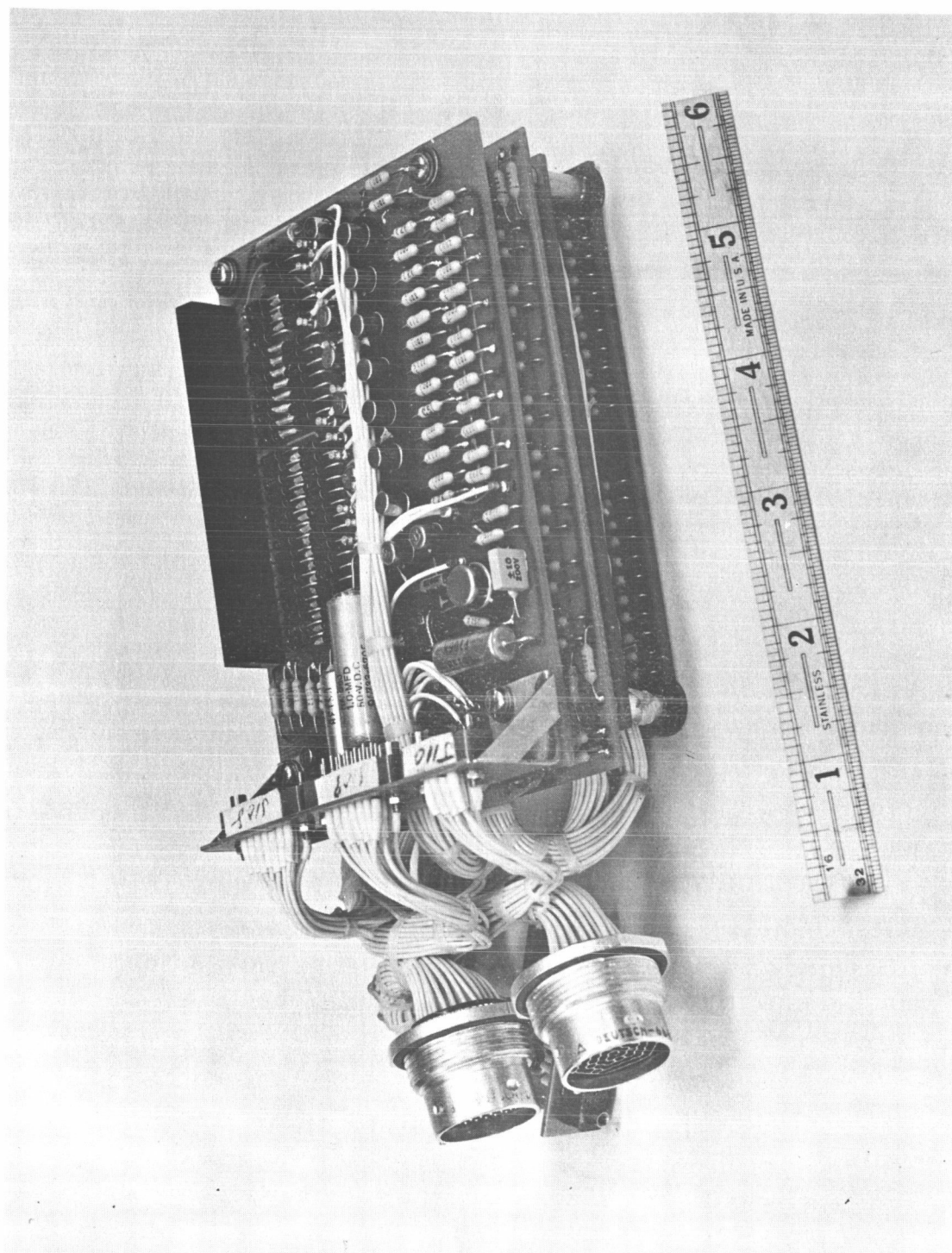


Figure 8. Aircraft Model Coil Current Readout Module

939/056

reasons (1) an improved signal to noise ratio is accomplished (2) angular resolution is improved by removing energy from the previous beam position.

The output of the integrate and dump filter is connected to the analog-digital converter (Block 12). Conversion time for the converter is on the order of 50 μ seconds. The output of the analog to digital converter is a parallel nine bit word plus parity that occurs every 200 millisecond. This is coupled to the parallel to serial converter (Block 13) which in turn couples to the telemetry system of the spacecraft digital recorder or bench test set.

The parallel to serial converter was originally included to interface with the NIMBUS Spacecraft telemetry system which could only accept a serial word.

The second output of the analog to digital converter is coupled to the stepped AGC circuitry (Block 7). This circuitry contains logic that compares the analog to digital converter output against a previously stored word. If the comparison results in a high or low difference that exceeds a preset threshold, attenuation is inserted or removed in series with the output of the 600 cps post-detection amplifier (Block 6). In order to identify the proper output word, ferrite switch number two is thrown to the cold reference horn (Block 19) at the end of every second scan. Now the second ferrite switch is switching between the hot reference load and cold reference horn at a 600 Hz rate. The operation of the radiometer is the same as previously described. Since the hot reference load and cold reference load are fixed, a known word should always result at the output of the analog to digital converter. This word is the word used to compare with the stored word in the stepped AGC logic. This word from the output of the analog to digital converter can change by gain changes in the radiometer amplifier chain. Thus, by inserting or removing attenuation every other scan, if necessary, the output word can be made to return to the same word stored in the stepped AGC logic. The maximum attenuation inserted or removed at one time at the end of every other scan is 1/2 dB. The total attenuation that can be inserted or removed is 32 dB.

For readout purposes of the stepped AGC attenuation setting, a parallel to serial converter (Block 9) is connected to the stepped AGC logic.

All power to the radiometer is controlled by the power command relay (Block 27). In the on condition a -24.5 Vdc power source is connected to the dc to dc converter (Block 26). The dc to dc converter operates from the 2400 Hz clock signal supplied from an external source. DC outputs of +4 Vdc, +15 Vdc and -15 Vdc are derived by the dc to dc converter.

The timing and control counter (Block 25) receives three signals from an external source 10 pps, 1 pulse/16 sec and 2400 pps. The timing and control counter receives these signals, converts them to new rates where necessary and provides outputs sufficient to drive all the circuits requiring timing signals.

The switch drivers are driven by a 600 Hz and a 1/16 pps signal. The switch drivers (Blocks 22, 23) are special amplifiers that drive the inductive load presented by the switches. Special damping and overshoot techniques are used in these amplifiers to prevent switch chatter.

The hot load consists of a stepped termination seated in a section of wave guide. The wave guide is seated in a copper block which contains heaters and heat sensors. The entire block is enclosed in an epoxy foam which provides insulation. The heaters and sensors are connected to a servo amplifier (Block 24) which controls the hot load temperature to within 0.1°C at 65°C .

The beam steering computer (Block 18) receives timing signals from the timing and control counter. It converts these signals to 5 pps which is the stepping rate of the antenna beam position. The computer sets the coil for each coil for a given position, since there are 49 coils and 39 discrete positions then there are 1911 discrete currents during one scan.

In order to read out the antenna coil currents an analog multiplexer (Block 16) connects one coil to the level converter with the position determined (Block 17) by status of +50 counter (Block 16) for 39 beam positions, then to the next coil for 39 beam positions and etc., until all coils have been connected to the level converter. The level converter performs the function of measuring the voltage drop across a sensing resistor in series with each phase shifter coil.

It does this function by connecting an amplifier to the high side of the resistor and then to the low side of the resistor. This is performed at a 600 pps rate. The square wave magnitude is directly proportional to the voltage across this resistor. By synchronous detection the square wave is converted to a dc voltage. This voltage is a measure of the coil current for that beam position. By chopping and ac coupling, the high quiescent voltage level at which the resistor is biased can be removed and only the voltage across the resistor is measured. This method was required by the constraint of the maximum voltage supplied by the main power source. Since it was -24.5 Vdc and the bias level was close to -24.5 Vdc sufficient voltage difference did not exist to dc couple a transistor to the resistor.

The beam steering computer receives timing signals at a 40 pps, 20 pps, or 5 pps rate. This signal drives a counter which is connected to a diode matrix (Block 15). The diode matrix decodes the counter state and connects an amplifier to 49 resistors each connected to a phase shifter. For each number decoded another amplifier is connected to another set of 49 resistors. Each time an amplifier and set of resistors are connected to the phase shifter a beam position is established. This process is continued thirty-nine times which corresponds to 39 beam positions, on the fortieth count, the framing counter is reset to one. Thus, the scan repeats itself.

The fail safe command relay (Block 21) receives a signal from the console or spacecraft telemetry. This signal causes a relay to be activated which disconnects the beam steering computer from the prime power source. The antenna receives no steering commands, the beam assumes a quiescent position which is approximately broadside. This feature was incorporated to provide flexibility in the equipment in case of a beam steering computer failure.

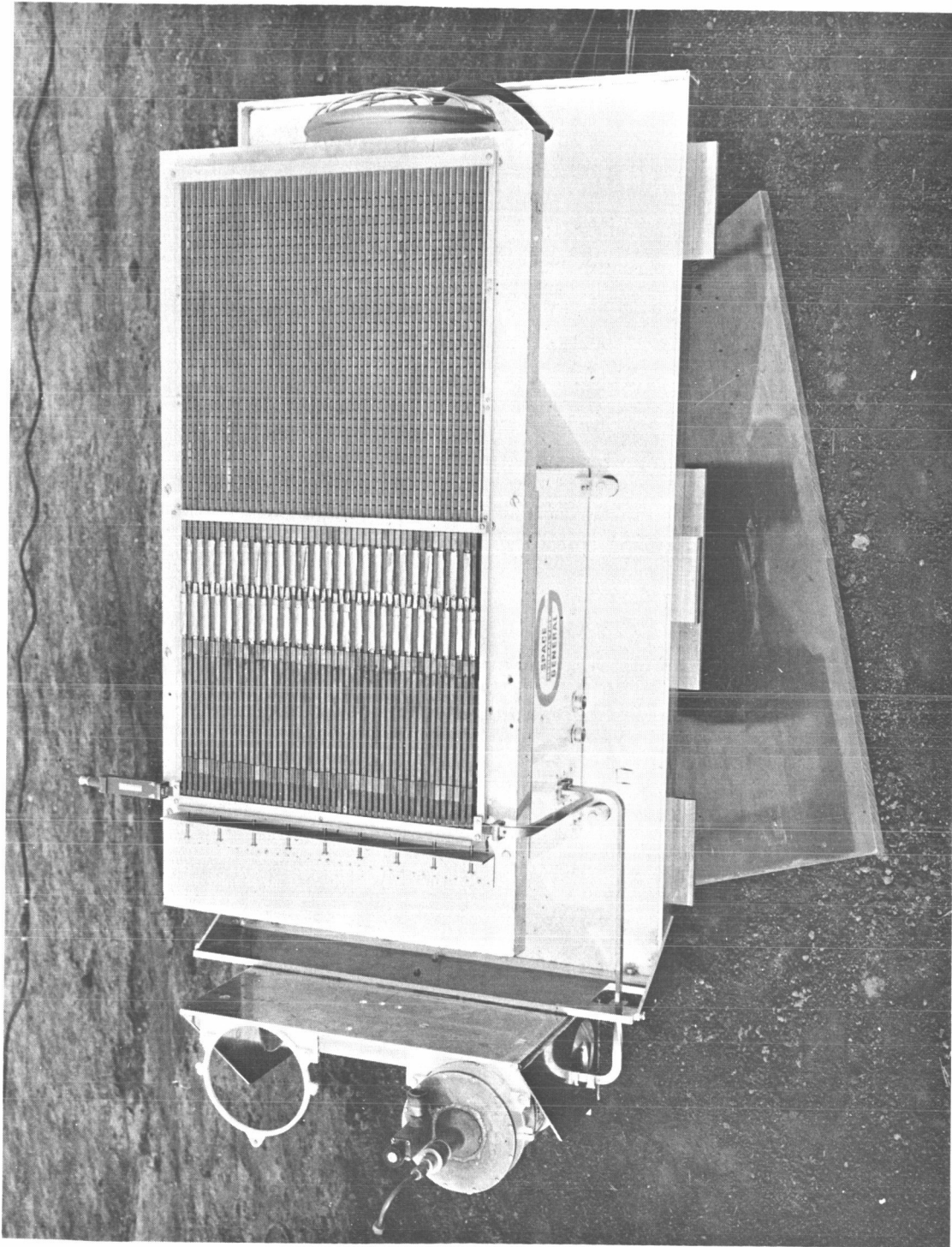
The timing and control counter guarantees a 600 Hz signal which drives the periodic switch and demodulator. The drive signals are synchronous thus allowing synchronous detection of the square wave signal from the second detector.

2.2 ANTENNA

The antenna consists of 49 edge-slotted waveguides, 36 slots/waveguide. The 49 waveguides are assembled into a planar array spaced approximately $1/2$ wave apart. Between each waveguide is a ground plane, spaced

approximately $1/4$ wave behind the slotted edge of the guide. The ground planes consist of aluminum extrusions bonded by silver loaded epoxy (Eccobond SG) to the waveguides (see Figure 9). Additional stiffness is achieved by aluminum members running perpendicular to the length of the waveguides. Further stiffness is achieved by an aluminum frame work around the entire antenna, phase shifter assembly, and feed. All cross members are epoxied to the waveguide and bolted to the antenna frame. At the farther end of each waveguide is a stepped load which matches the waveguide characteristic ($VSWR < 1.06$) impedance over the band of frequencies for which the system was designed, in this case from 19.15 GHz to 19.55 GHz. The stepped load is incorporated into each waveguide to absorb the remaining energy that is not radiated out through the 36 slots. Connected to each waveguide is a Reggia-Spencer phase shifter. By adjusting the phase shift of each phase shifter in the proper manner, the beam shape can be maintained and positioned to 39 discrete beam positions over $\pm 50^\circ$ from antenna broadside. The Reggia-Spencer phase shifter consists of a section of waveguide with a "rolling pin" shaped piece of ferrite material held at each end by Teflon blocks. The Teflon blocks are tapered at both ends to provide impedance match to the characteristic impedance of the waveguide. A coil of No. 36 formvar wire is wound around the outside of the waveguide and positioned over the ferrite located inside the waveguide. By passing current through this coil, a magnetic field is established which in turn changes the permeability of the ferrite material. With a change in permeability the velocity of propagation changes resulting in a phase shift of the energy as it passes through this section of waveguide. By driving each of these coils with the proper current in time sequence, the beam can be steered. In this system drive is obtained by a beam steering computer.

Connected to each phase shifter is a length of waveguide that is used to separate the phase shifter and feed. In the process of designing and testing this antenna, it was found the phase shift versus current characteristics of the phase shifters were affected by the proximity of the phase shifters to the feed slots. Phase shift versus current was not predictable until physical separation was accomplished. Upon solution of this phenomena, investigation did not continue, but it was hypothesized that several modes of propagation were established by the slot coupling of the feed. This additional path length was needed to attenuate



939/017

Figure 9. Breadboard Radiometer and Phased Array

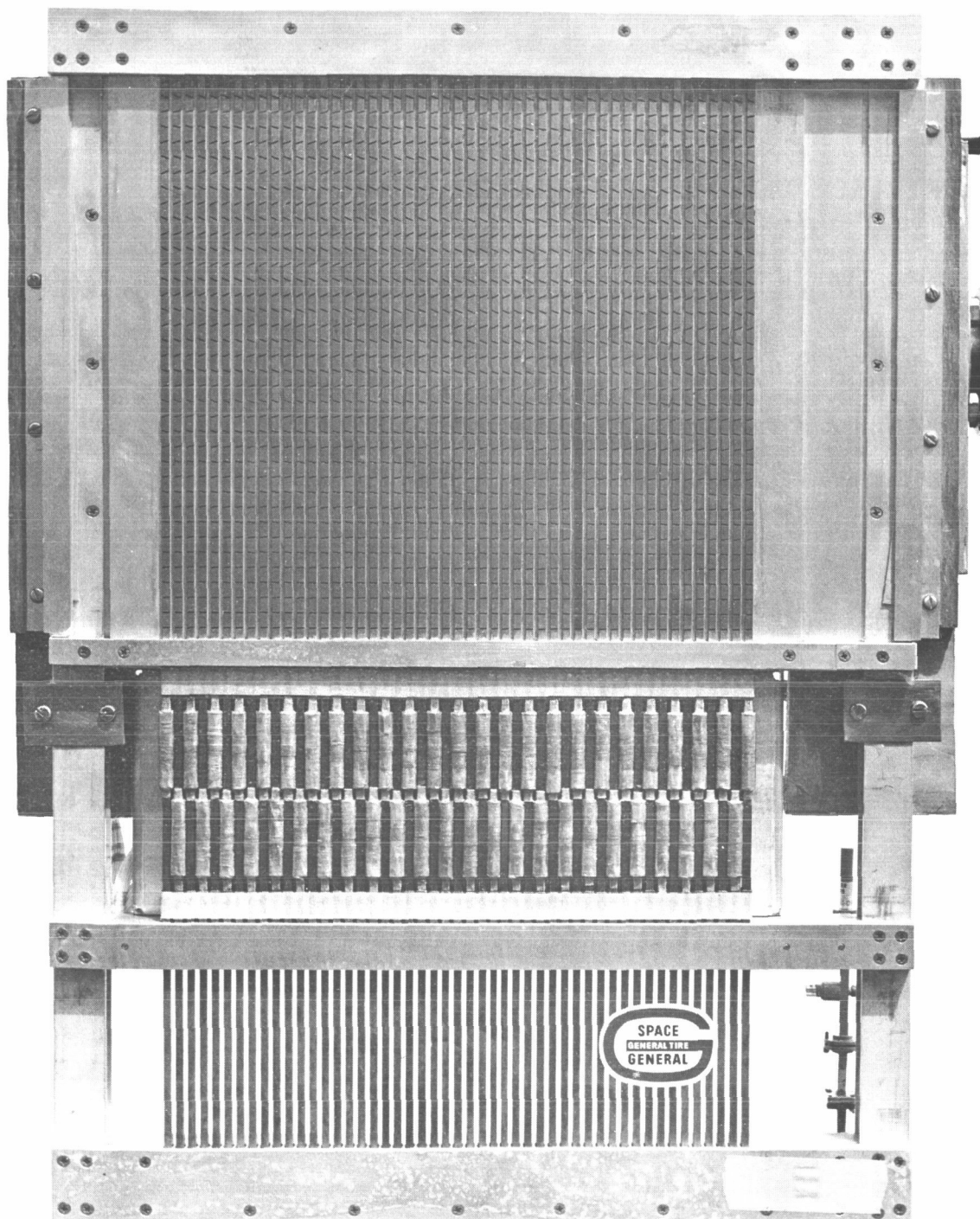
these undesirable modes. Optimum length of separation was not rigorously established.

The feed consists of an edge-slotted waveguide, each slot feeding one of the 49 waveguides in the planar ensemble. At the one end which is opposite from the feed end of the feed, a stepped termination like that in each planar array is incorporated into the feed. The termination material is Radite 75. The termination impedance matches the open end of the waveguide to the characteristics impedance of the waveguide over the band of frequencies for which the system was designed, namely; 19.15 GHz to 19.55 GHz. Any energy that has not been radiated through the slots in the feed to the planar arrays is absorbed into this load.

Coupling of the pieces (phase shifter, antenna, waveguide spacer and feed) is accomplished by butt joints and sleeves, the sleeves sized for a press fit and epoxied in place. The aircraft antenna is shown in Figure 10. Since the breadboard was designed for the NIMBUS orbit of 600 nautical miles, the scan time was selected to give 3 dB overlap in the down track path. For the Convair 990 aircraft the velocity over height ratio changed drastically to the point that large gaps in the scan coverage would appear in the down track path. It was determined that to optimize the system, the aircraft could fly at two altitudes, namely 9,000 feet and 24,000 feet. At these altitudes the scan rates were determined to be one second and two seconds, respectively. Systems performance deteriorated accordingly, since the scan angle had to be traversed in $1/4$ and $1/8$ the time it previously had. The ΔT of the system went up from 0.7°K to 1.1°K and 1.5°K .

Tradeoffs were necessary, and it was the opinion that a larger ΔT could be tolerated gaining an increased angular resolution and getting down track coverage at the 3 dB points. Further targets became more beam filled and in some cases offset the reduced sensitivity. Subsequent tests aboard the Convair 990 aircraft bore out the adequacy of the systems tradeoffs mentioned above.

The antenna for the aircraft model was significantly different from a mechanical standpoint. The breadboard antenna was fabricated by epoxying waveguide to aluminum extrusions as ground planes. In the case of the aircraft model,



939/053

Figure 10. Aircraft Antenna

the ground plane structure consisted of a honeycomb sandwich of aluminum plate. Channels were milled out on one side to receive the planar arrays with the remaining material acting as ground planes. Each planar array was epoxied to the sandwiched honeycomb structure. Additional stiffness was achieved by framing the entire structure. This framing was designed to receive the Rexolite radome. To improve the insertion loss in the aircraft model antenna, one joint was eliminated by coupling to the feed with a waveguide section of significant length to isolate the phase shifter from the slot coupling of the feed. On the breadboard antenna, this section was two pieces coupled by a sleeve. This was one of the main factors in reducing the antenna loss. Additional factors entering into the reduction were aligning the waveguide sections and phase shifters with the antenna by using the same precision tooling used to fabricate the antenna. Butt joints of each of the components (feed, phase shifter, and antenna) were machined to be flat and parallel to ensure minimum gap when butted together.

The aircraft antenna was designed to be considerably heavier than the breadboard antenna. Aircraft use dictated heavier design, since weight is not a limitation on aircraft whereas on spacecraft it is of prime importance. After initial shock and vibration, due to launch, spacecraft instrumentation is not subject to further shock or vibration. Contrary to this aircraft instrumentation is subjected to prolonged shock and vibration, repeated for every flight. Therefore, aircraft antenna was designed to be considerably stiffer and more rugged and consequently resulting in more weight.

Heaters and a purge system were added to the antenna to prevent condensation in and on the antenna and to prevent the ferrite phase shifters from becoming inoperative due to low temperatures encountered at high altitudes. Pressurization was supplied from two parallel connected nitrogen bottles with pressure regulators set at 32 lbs/sq. inch. Flow and pressure were regulated by a sonic and subsonic orifice respectively. These orifices were chosen to regulate the pressure on the radome to a relative constant pressure regardless of altitude. The ferrite phase shifters were never tested below -10°C , therefore, performance could not be predicted below -10°C . It was decided to install heaters, fly without energizing the heaters, and assess performance of the antenna. Based on the outcome of this test, the heaters would or would not be energized. Flight

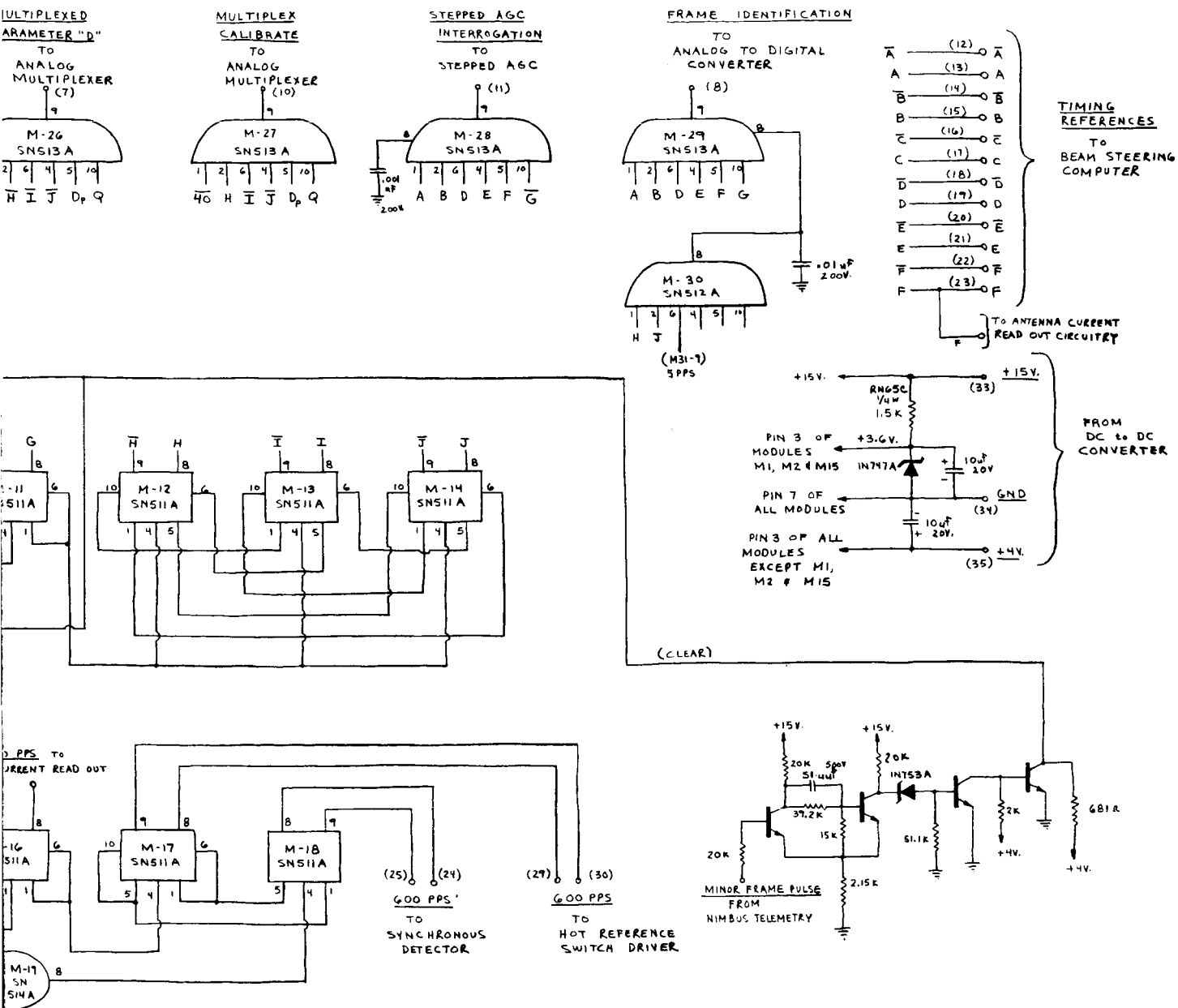
data indicated no degradation in performance of the antenna for all temperatures encountered on the flight. Temperatures encountered on the antenna as monitored by thermistors were as low as -20°C . The entire flight test was performed without energizing the heaters.

Seven thermistors were mounted on the antenna to determine antenna temperatures and gradients along and across the antenna. It was determined that no gradients were measured within the two percent accuracy of the monitoring equipment. The purpose for monitoring these temperature gradients across the antenna and phase shifters, especially the phase shifters, is that mechanical and electrical characteristics change resulting in phase perturbations which give rise to a reduction of beam efficiency and beam position accuracy. Fortunately because of a large heat sink to the aircraft and the radome, gradients were not detected. The radome, in a radiometric sense, introduced losses of 0.03 dB at the broadside position and 0.1 dB at the 50° point. Patterns were affected very little as shown by the patterns in Figure 11 with and without radome. The counter and control block diagram is shown in Figure 12.

2.3 DICKE SWITCHES AND HOT AND COLD LOADS

Referring to the block diagram, Figure 1, Blocks 1, 2, 19, 20, 22, 23, and associated auxiliary blocks constitute the portion of the system which performs the function of switching the receiver input (Block 4) between the antenna and the calibrating sources. The details of this switching function are covered in Appendix XXIV.

The signals from the antennas and the hot and cold loads are applied to a balanced 19.35 GHz mixer, combined with the LO signals (Block 5) then the resultant signal is applied to the IF amplifier (Block 4), square law detector and post-detection amplifier (Block 6), synchronous detector, and then on to the data processing and display circuitry.



Schematic Diagram

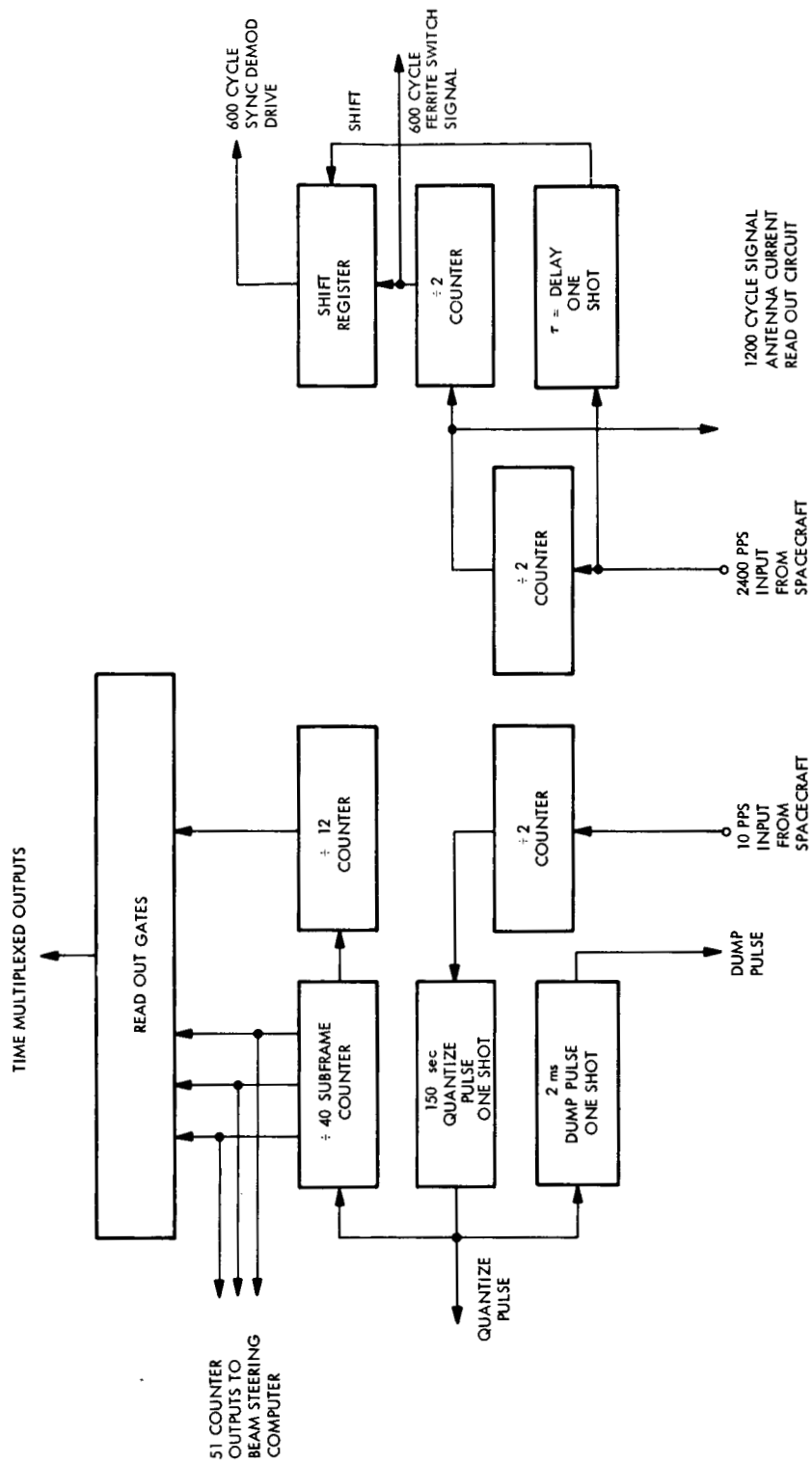


Figure 12. Timing and Control Counter, Block Diagram

2.4 RECEIVER

The initial design plan for the radiometer receiver was to be a tuned RF amplifier using tunnel diodes in cascade to give the desired amplification. Tunnel diodes at this frequency were to be obtained from a single commercial source, and were to be hand selected from a given production run. Failure to achieve the given tunnel diode characteristics, at this time, by the other commercial source, forced Aertech Corporation, who was contracted to build the tunnel diode amplifier, to use inferior diodes. The result was a tunnel diode amplifier that was inferior to the specifications.

Accordingly, when it became evident that Aertech Corporation could not supply the subcontracted tunnel diode amplifier to specifications, Space-General undertook an effort to develop and build a solid-state superheterodyne double sideband receiver.

This receiver configuration now consists of ferrite switches arranged in one package, an isolator, balanced mixer, solid-state local oscillator, solid-state multiplier, synchronously tuned IF amplifier, square law detector, preamplifier, and synchronous detector (see Figures 13 through 17).

Dicke switch characteristics for the breadboard were 1 dB of insertion loss, 20 dB minimum of isolation during the worst switching conditions, drive current of 120 ma at 24.5 V and switching time of 120 microseconds. The overall noise figure of the receiver, measured with ten different sets of crystals, varied between 5.0 dB and 6.0 dB, double sideband noise figure.

The IF amplifier bandwidth was 200 MHz with a center frequency of 120 MHz. The IF amplifier and video preamplifier were packaged in one unit to provide RFI integrity. Thus, signals emanating from the IF preamp package would be of sufficient magnitude to override interference signals should they be present. The IF gain was 57 dB, detector responsivity was 17 volts per milliwatt, preamp gain was 57 dB, and a mixer conversion loss of 6 dB to give a sensitivity of 5.85 microvolts per degree Kelvin.

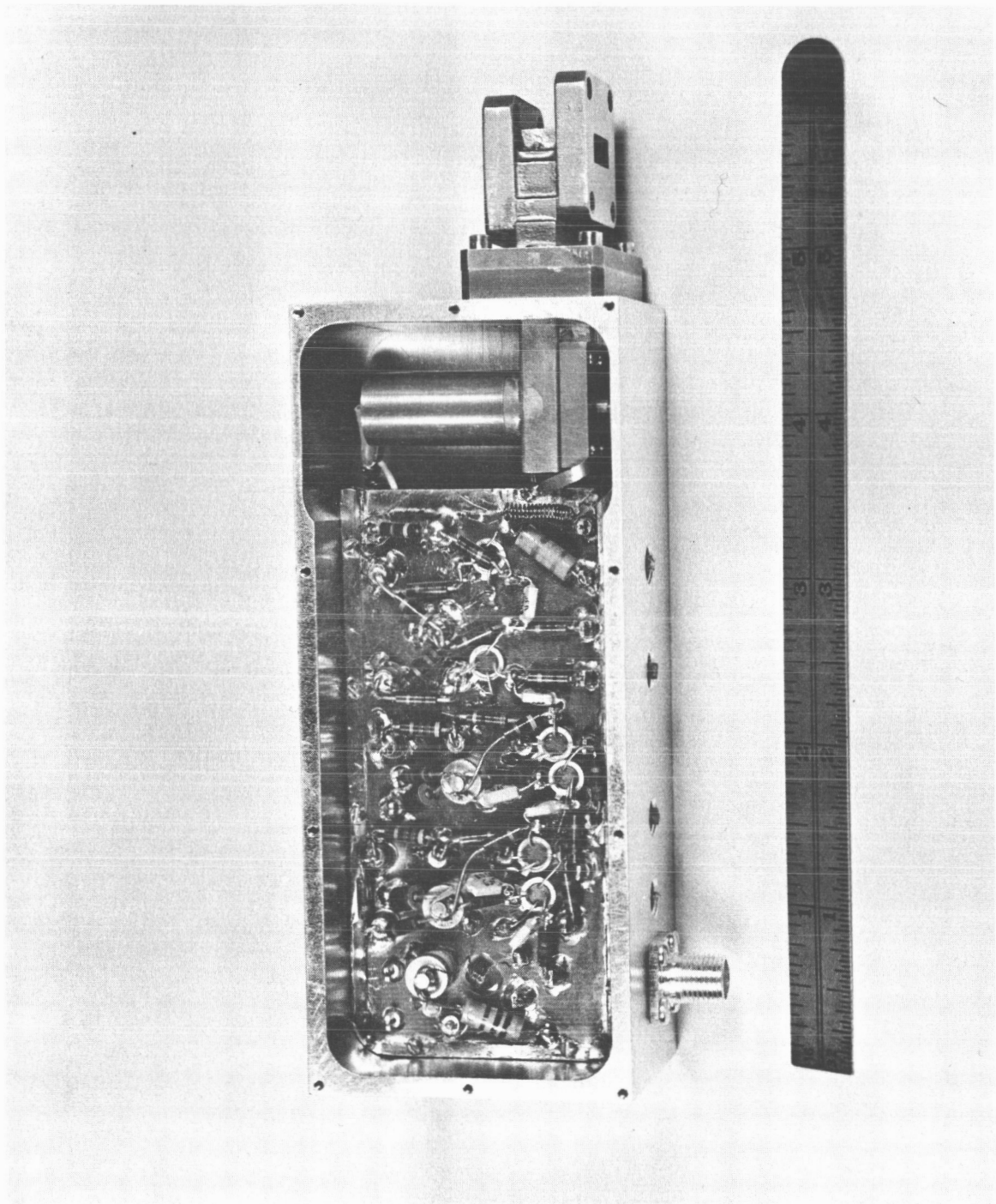
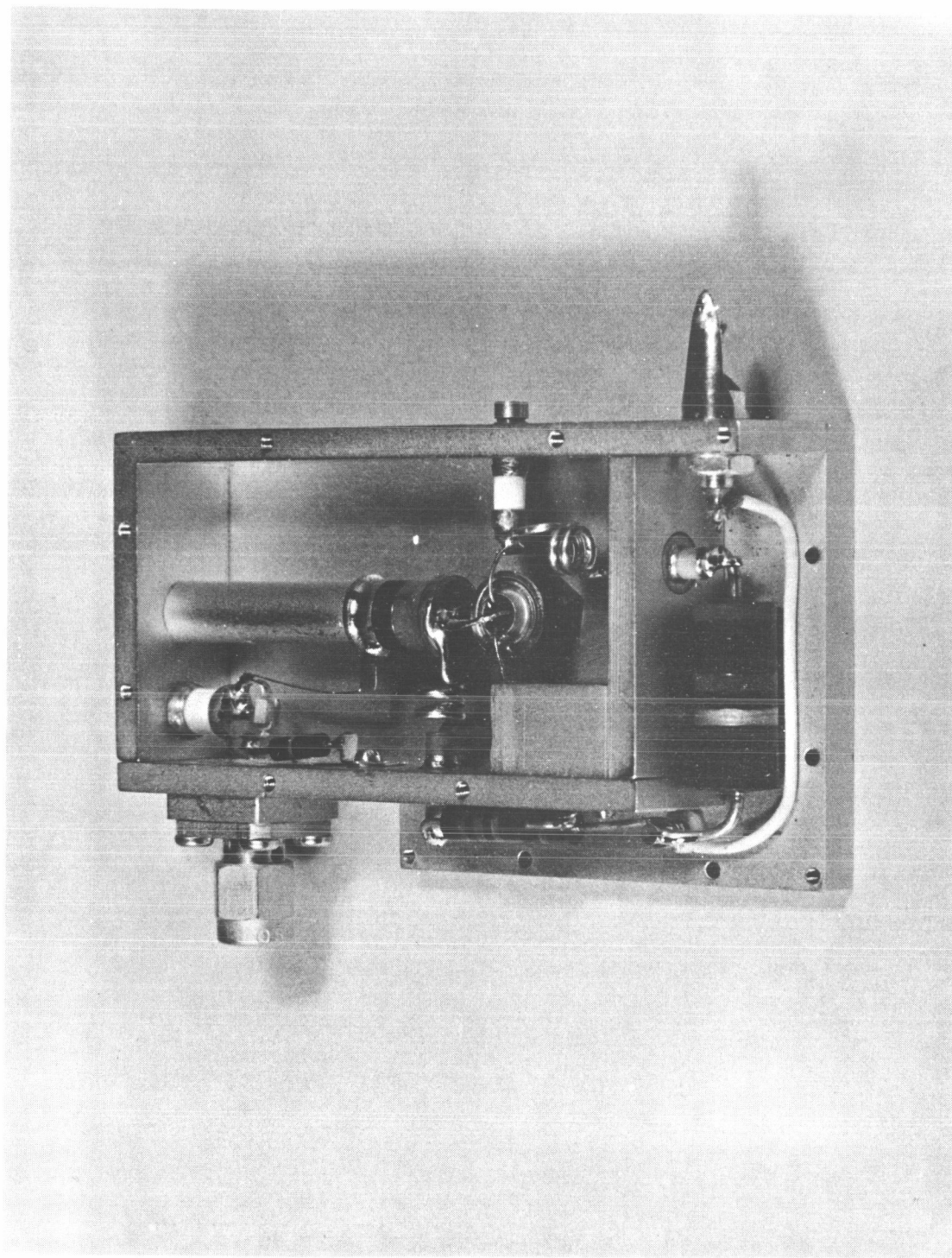


Figure 13. Mixer IF Amplifier



939/035

Figure 14. Solid-State Local Oscillator, Aircraft and Breadboard

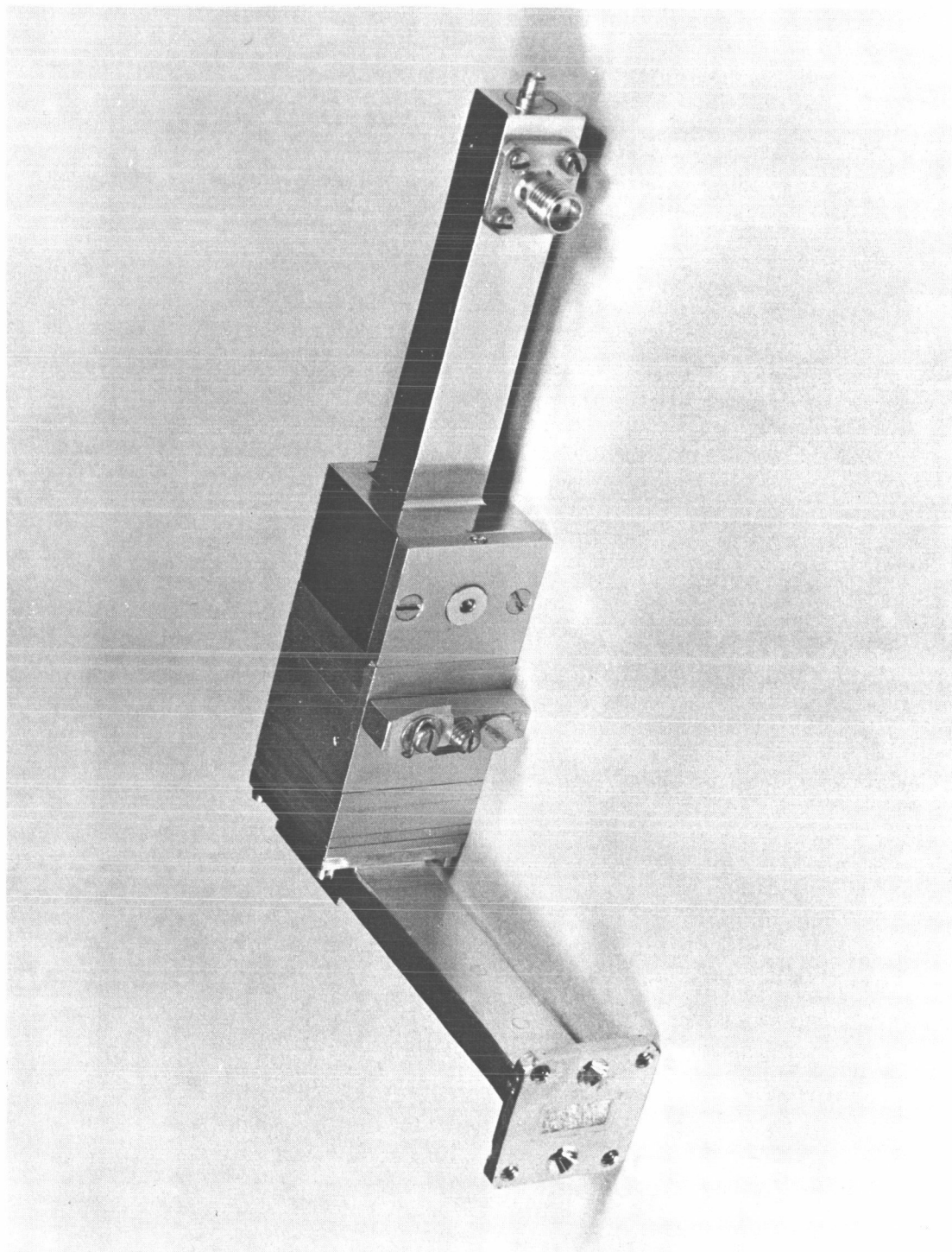
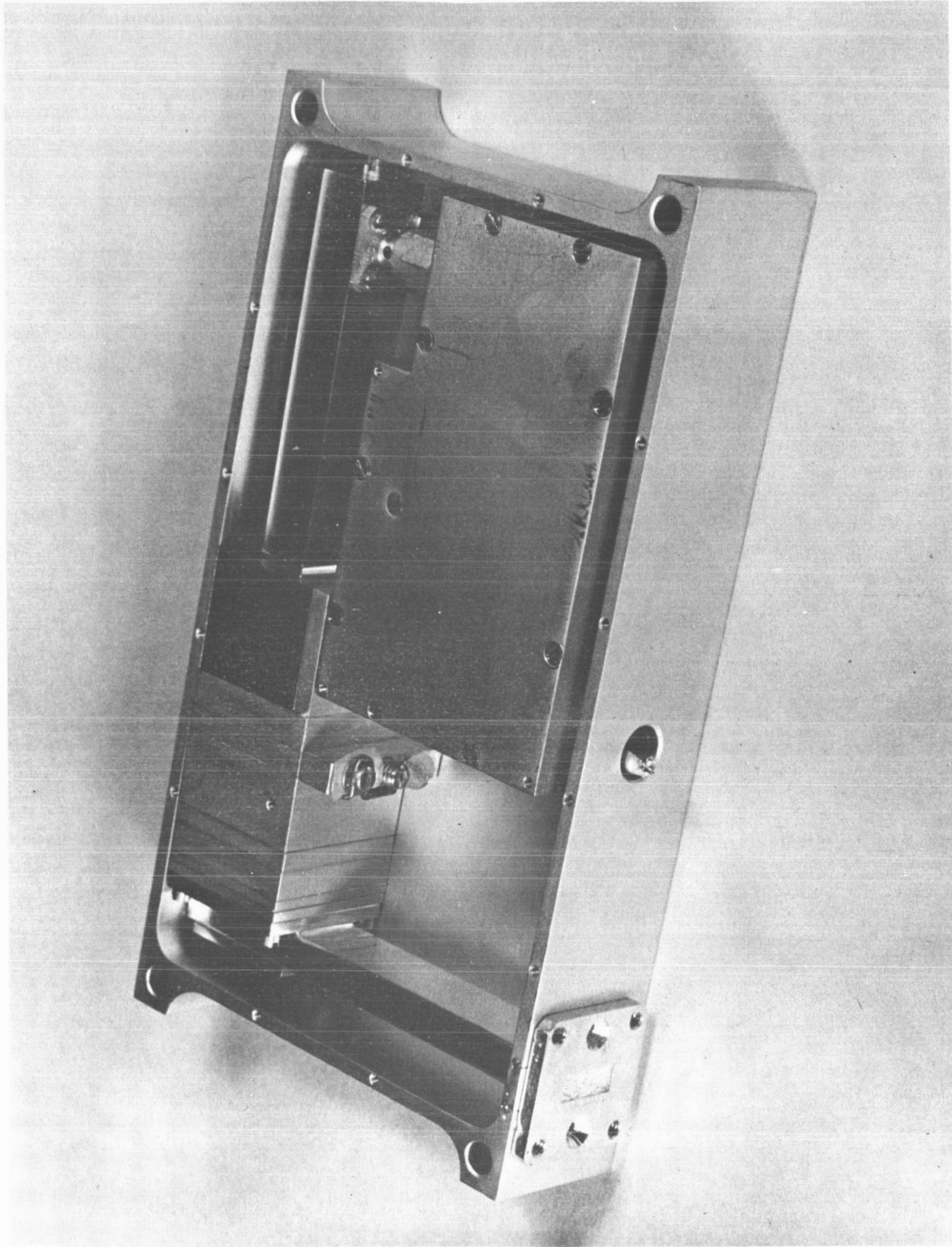


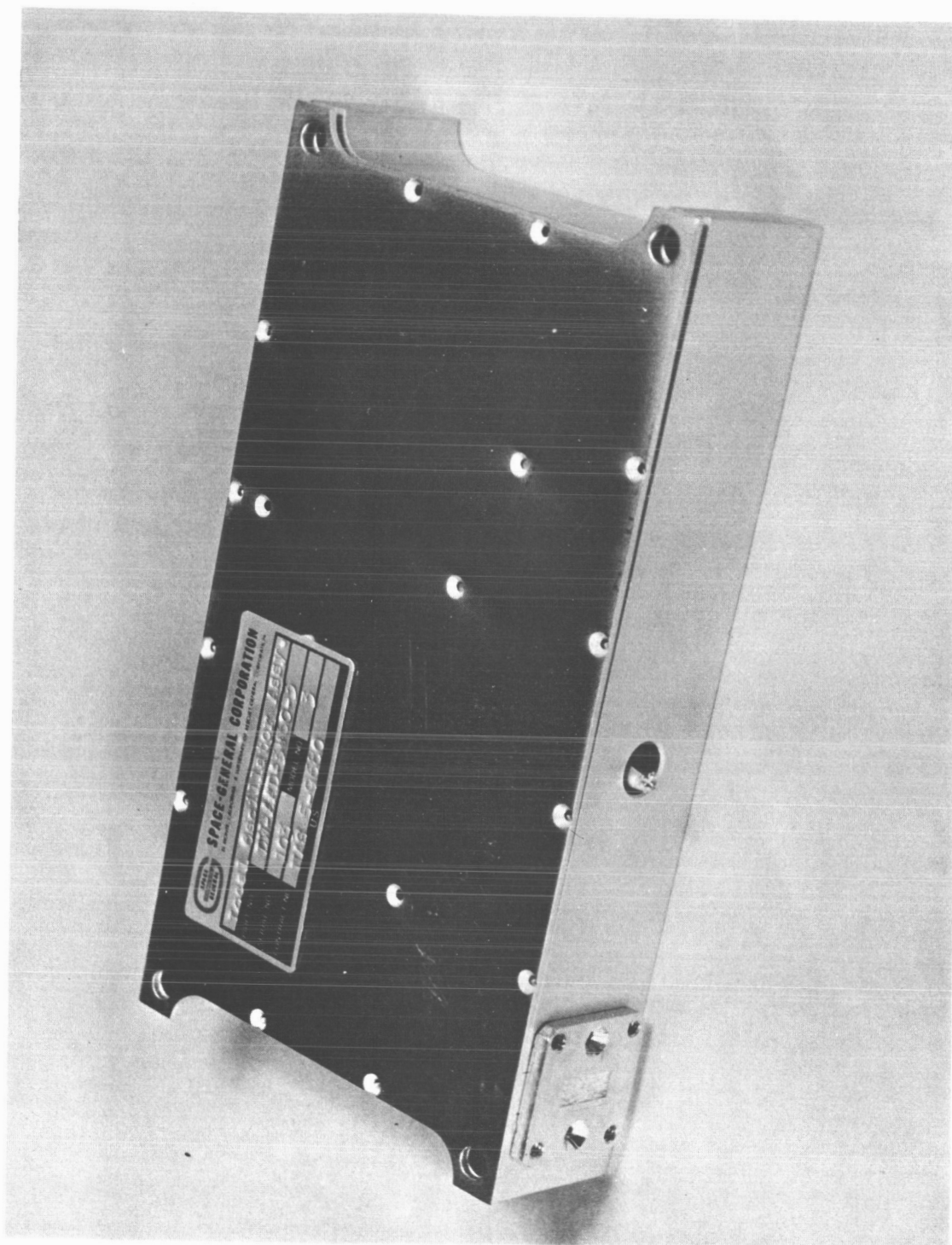
Figure 15. Solid-State Multiplier

939/036



939/037

Figure 16. Solid-State Source, Aircraft and Breadboard



939/038

Figure 17. Solid-State Source, 19.35 GHz, Aircraft and Breadboard

$$\text{Sensitivity} = KT \, \delta \, G \gamma$$

$$\text{Sensitivity} = 1.38 \times 10^{-23} \times 1 \times 200 \times 10^6 \times 17,000 \times 1.25 \times 10^5$$

$$\text{Sensitivity} = 5.85 \, \mu\text{V}/^\circ\text{K}$$

where

K = Boltzman's constant

T = Temperature in degrees Kelvin

δ = Predetection bandwidth in CPS

γ = Second detector responsivity in volts/watt

G = IF gain plus conversion loss

Nominal gain for the video preamp was 40 dB and for the post amplifier synchronous detector the gain was 40 dB.

There were several changes in the digital circuitry that were imposed as the result of the design review held at GSFC during February 1966. These were a parallel to serial converter as a result of a change in the telemetry format imposed by GSFC. A two to one count down circuit, to count down from 10 PPS to 5 PPS in the timing and command signals from the spacecraft. Originally, a 5 PPS timing signal was to be supplied by the spacecraft, but later information indicated and confirmed only a 10 PPS signal was to be available. A mode of operation was imposed whereby coil currents from the antenna could be read out through the digital output circuitry of the radiometer to the spacecraft telemetry link. This format was chosen to be such that one coil would be connected to the digital read-out circuitry for 39 beam positions or one scan. During the next scan the next coil would be switched to the digital readout circuitry for 39 beam positions. This procedure would continue until all coils had been switched to the digital output circuitry. A total elapsed time of 392 seconds is required to readout all coil currents for all beam positions. One other condition imposed as a result of the design review meeting was circuitry should be made available to readout in analog form the stepped AGC count to the spacecraft telemetry.

As a result of these changes, additional volume was required to house the new circuitry. A request was made of the technical officer at GSFC to increase the package size from a 2/2 NIMBUS module to a 4/4 NIMBUS module. The request was granted thereby increasing the radiometer volume by two for the prototype and flight models.

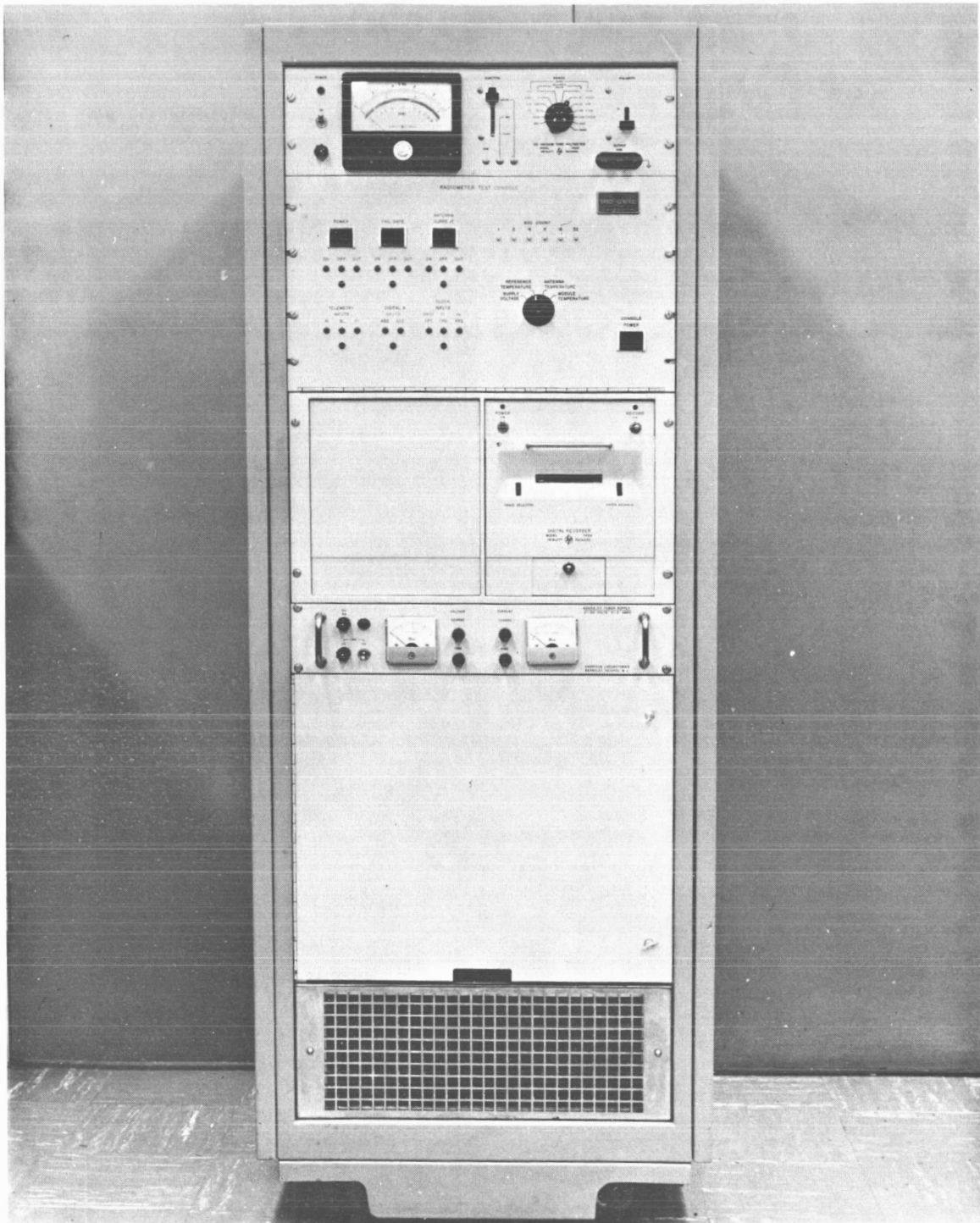
The original design proposed for the beam steering computer was followed during the course of the program with but minor expectations, such as, isolation diodes were used to isolate each current weighting resistor from every other current weighting resistor.

2.5 BENCH TEST EQUIPMENT

Two sets of bench test equipment were designed for this program. A bench test set consists of a console of equipment and a two-port cryoflask (see Figures 18, 19, and 20). A single port cryoflask is shown in Figure 21.

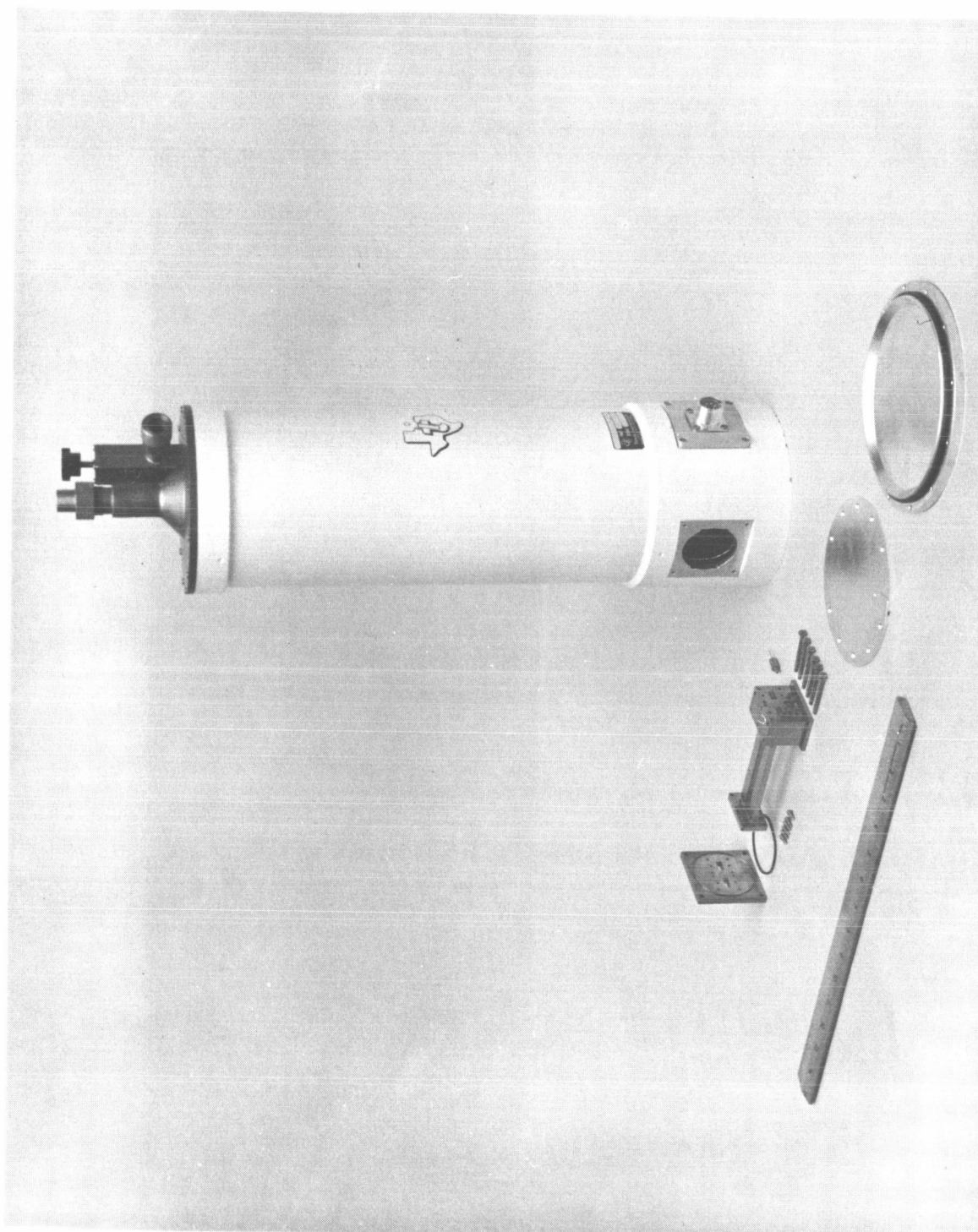
The bench test equipment was designed to supply timing signals identical to those of the spacecraft, supply power as normally supplied by the spacecraft, receive the output signals of the radiometer, and process these signals for visual readout on the rack displays. The radiometric output temperatures and multiplex parameters are processed by the bench test equipment and readout by a printer for each beam position. Stepped AGC count is readout on the console by a series of lights which display the count in binary form. Analog parameters are readout by a VTVM which can be switched by a knob to any analog parameter available. The various modes of operation are, fail safe, scan, or antenna current readouts, and are controlled by push buttons on the front panel of the console. Provided with the bench test console are three cables necessary to operate the radiometer. Storage space is provided in the console for these cables when the bench test equipment is not in use. Monitoring jacks are also available on the front panel for monitoring all timing signals.

The two-port cryoflask normally is filled with liquid nitrogen and cools a microwave load to liquid nitrogen temperature. The radiometer is coupled to the cooled load by means of two waveguide sections. One section couples directly to the sky horn port of the radiometer. The other section couples from the cold load through a variable attenuator to the scanned antenna



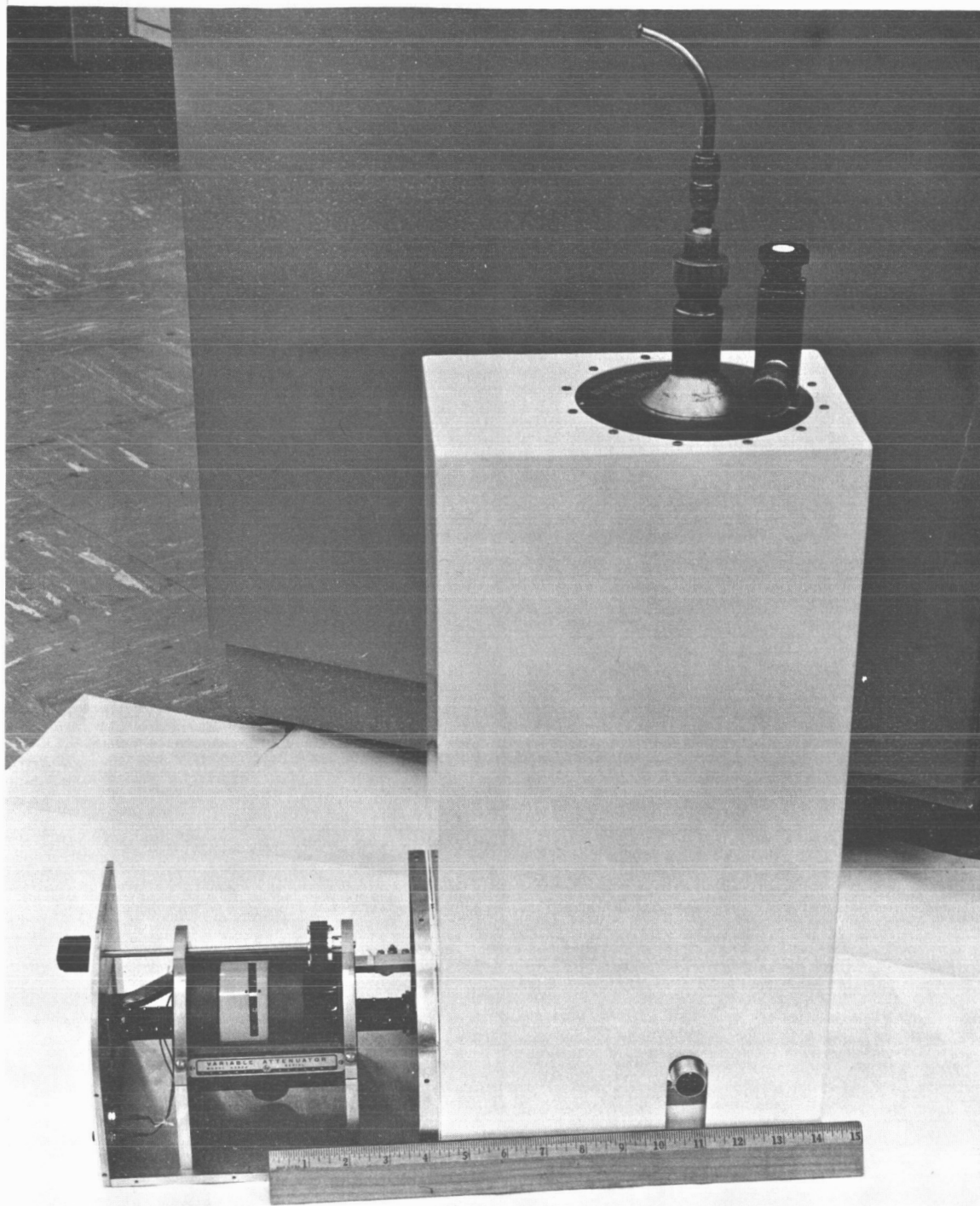
939/062

Figure 18. Bench Test Set Console



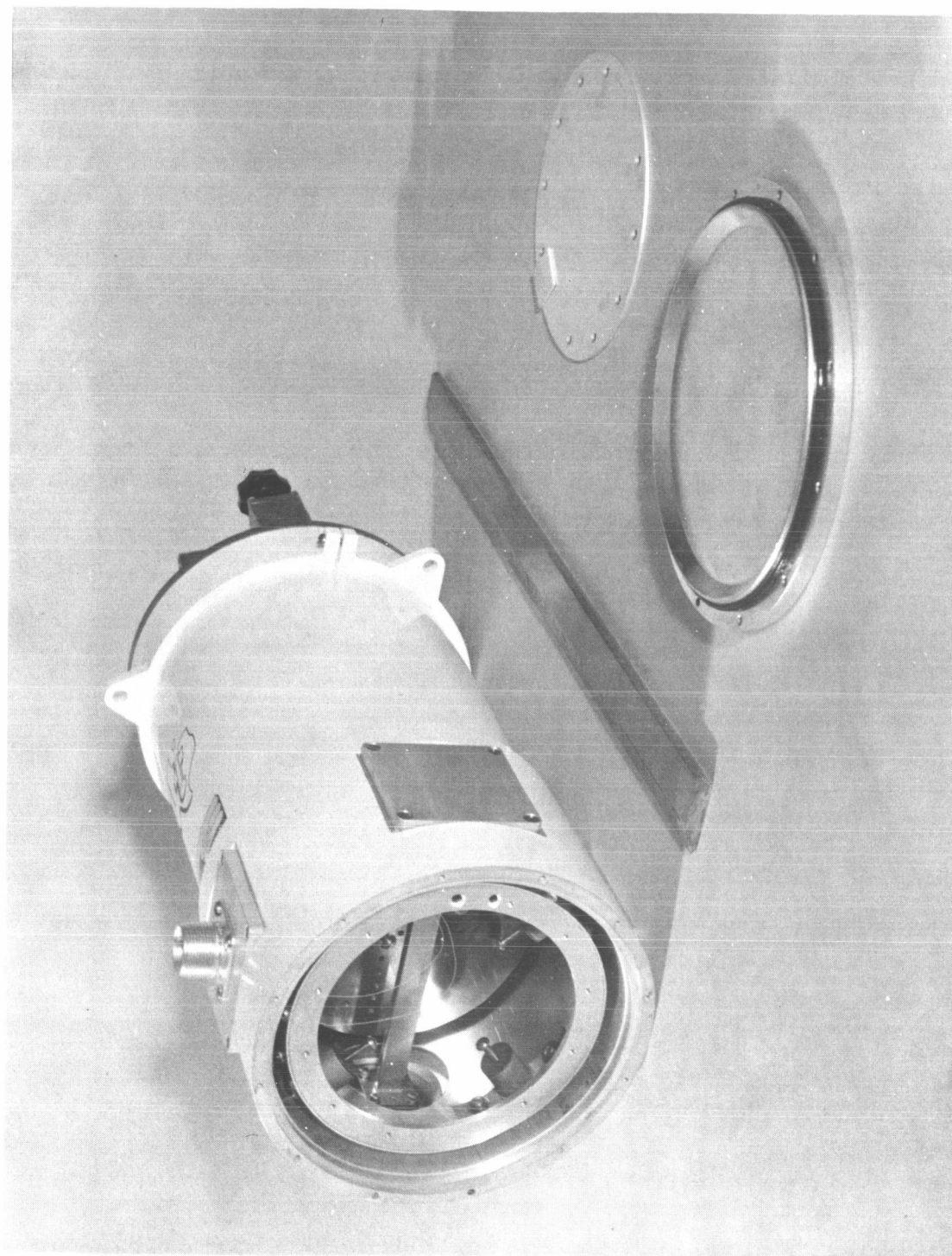
939/051

Figure 19. Cryogenic Equipment, Bench Test Set, Two Port



939/058

Figure 20. Cryogenic Bench Test Set, Two Port



939/049

Figure 21. Cryogenic Equipment, Aircraft Model, Single Port

port. The direct coupled section provides the low end point of the radiometer dynamic range. The variable attenuator section provides points from the low end to room temperature by adjustment of the attenuator attenuation. This provides a means of obtaining a calibrated transfer characteristic of the radiometer.

By means of a bench test set console, liquid nitrogen, and a 110 V ac 60 Hz power source the entire radiometer system can be exercised external to a spacecraft.

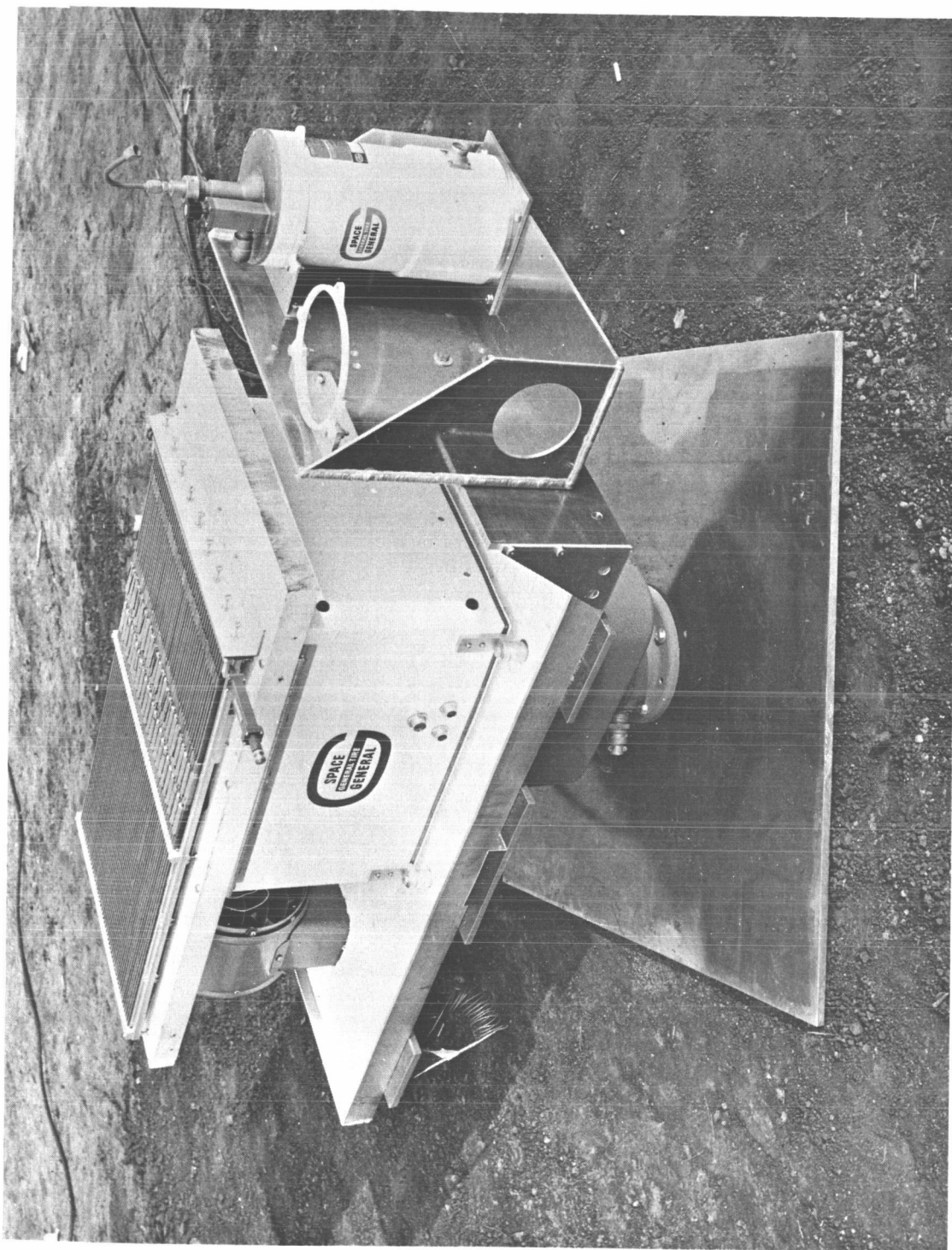
Tests were run at the Space-General plant, prior to the tests which were conducted at Table Mountain (see Figures 22 and 23). Also, the complete radiometer was tested on the antenna range prior to the Space-General plant tests (see Figure 24).

2.6 TABLE MOUNTAIN TESTS

By January 1967 the breadboard was constructed, debugged and checked out. Plans were formulated to take the radiometer system to Table Mountain, California, where JPL has test site facilities, and perform measurements on the system in a radiometric mode. A complete description of these field tests is given in Appendix XXIV.

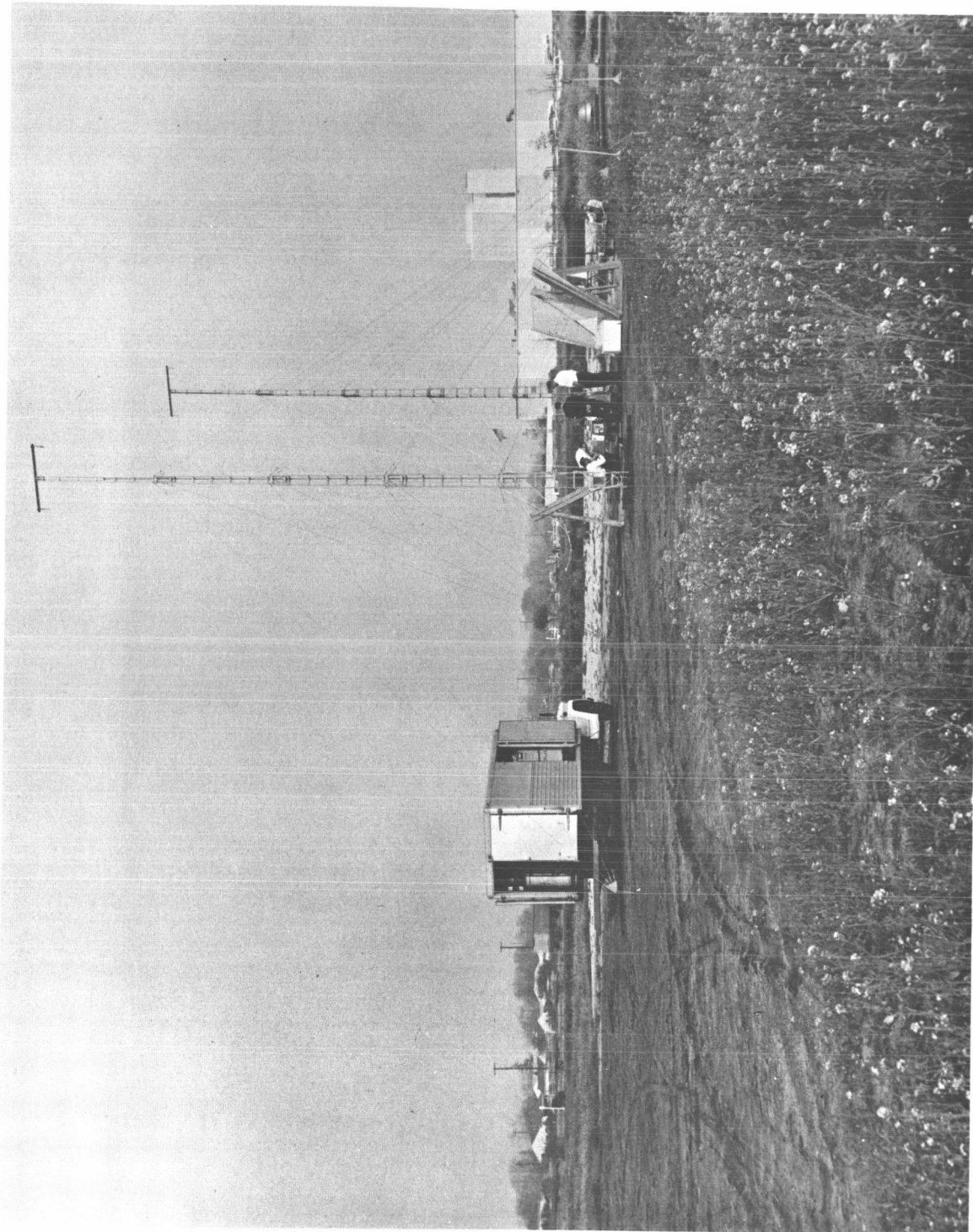
Two significant items that would effect the aircraft model came out of these tests. One, the antenna losses were too high, and two, the solid-state source for the receiver would not operate properly above 40°C. Figure 25 shows the equipment being set up for this beam efficiency measurement.

Several causes for the excessive loss in the antenna were postulated. The main cause was thought to be the three butt joints used to connect the feed to the phase shifters to the antenna. It was suggested that one butt joint be eliminated and more precision be used in making the butt joints as well as aligning the waveguide sections and phase shifters. As a result of these suggestions, the losses were reduced by 0.85 dB for the aircraft model antenna. The solid-state source instability was immediately diagnosed as a resistance change in the varactor diode bias. This resistor was compensated for by a thermistor. Temperature tests were performed on the solid state source. Operation within specification was obtained from -10°C to +60°C. This change was also implemented in the aircraft model.



939/023

Figure 22. Breadboard Radiometer and Phased Array Tests at Space-General



939/015

Figure 23. Field Test at Space-General Plant



939/054

Figure 24. Aircraft Model Antenna Test Boom (on Space-General Antenna Range)



939/043

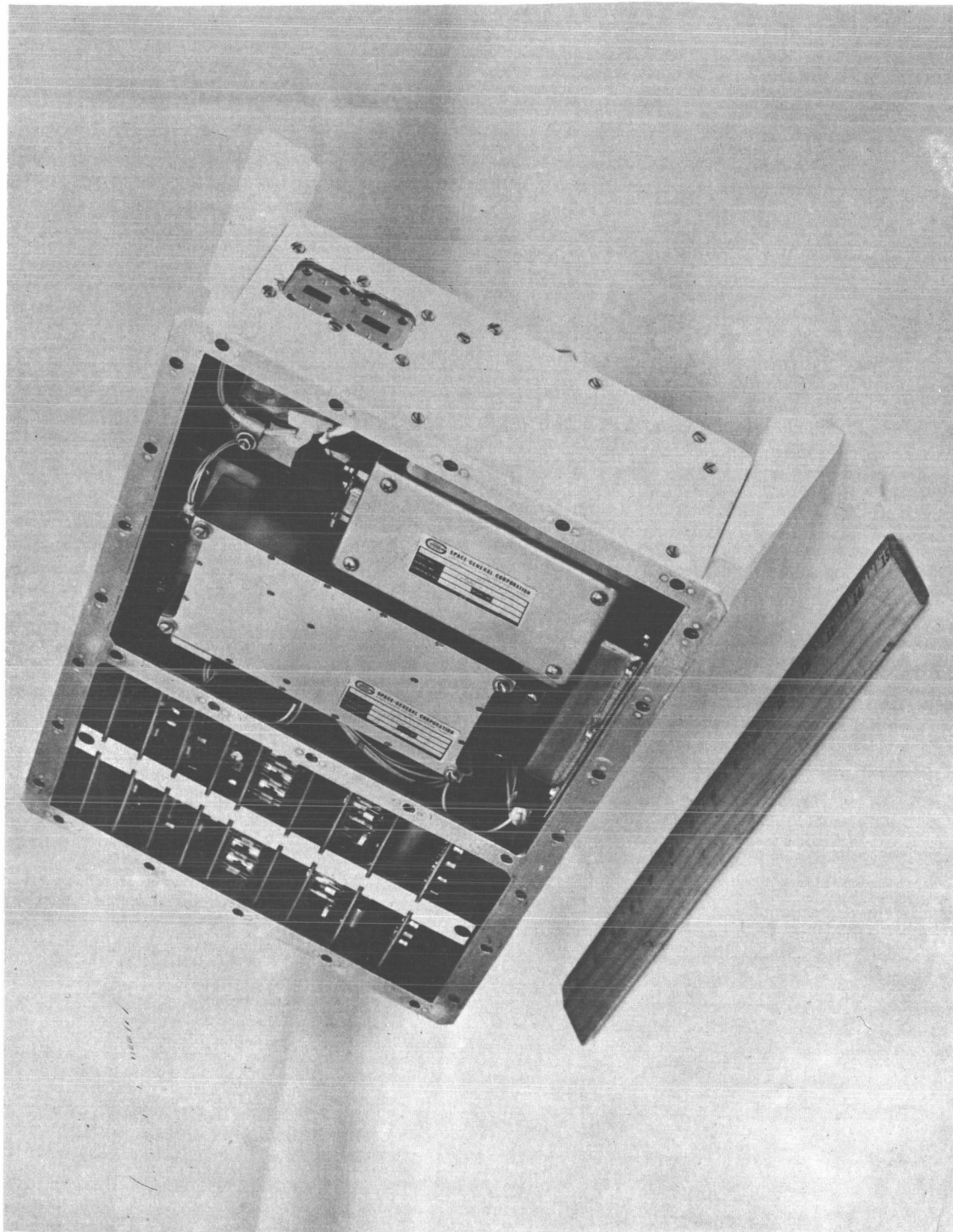
Figure 25. Table Mountain Beam Efficiency Measurement

2.7 AIRCRAFT MODEL

On February 1, 1967, contractual direction was given to Space-General to proceed to fabricate a radiometer system for A/C use that would provide maps in real time as well as record information on magnetic tape in digital form. The significant difference in appearance between the breadboard system and the aircraft system was size and construction. The breadboard system size was 20' x 14' x 14", whereas, the aircraft system was a 4/4 NIMBUS Module which is 6' x 8" x 13" (see Figure 26). The antenna incorporated a radome and mounting structure, the bench test set was replaced by a data acquisition system. This system occupied a rack supplied by GSFC designed and built strictly for aircraft use.

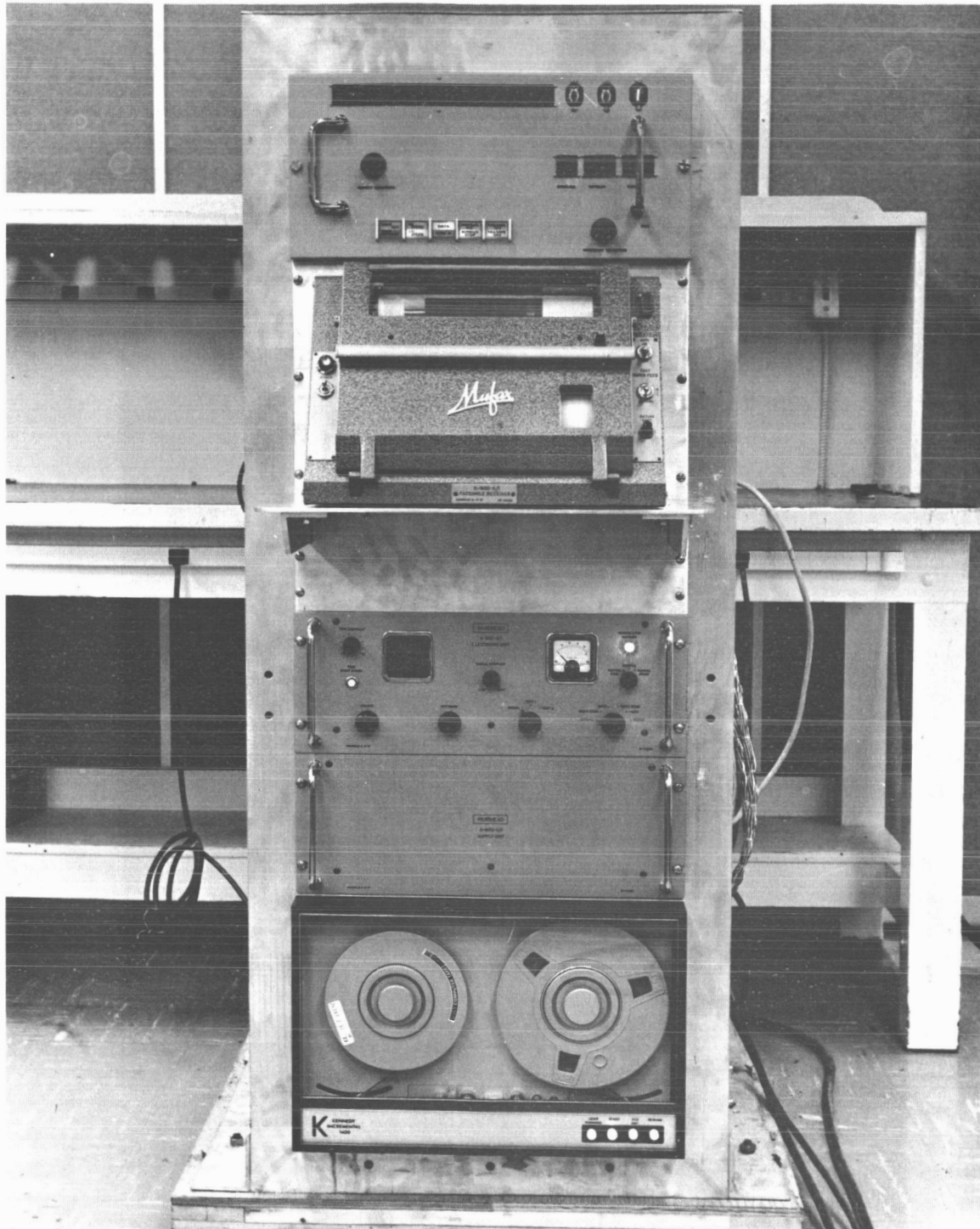
The data acquisition system consists of control and data processing electronics, power supply, facsimile machine, and digital tape recorder (see Figure 27).

The control and data processing electronics perform the same functions as the bench test set. However, since the scan time has been decreased the printer was replaced with nixie tubes for a visual readout. Printer response time was too slow to follow the scan rate. In addition to performing the same function as the bench test set the data acquisition system supplied control signals to the tape recorder and facsimile as well as processed the data in the proper format for the facsimile machine and tape recorder. A block diagram is shown in Figure 28.



939/059

Figure 26. One Half of 4/4 Aircraft Module



939/064

Figure 27. Aircraft Flight Recording and Digital to Analog System

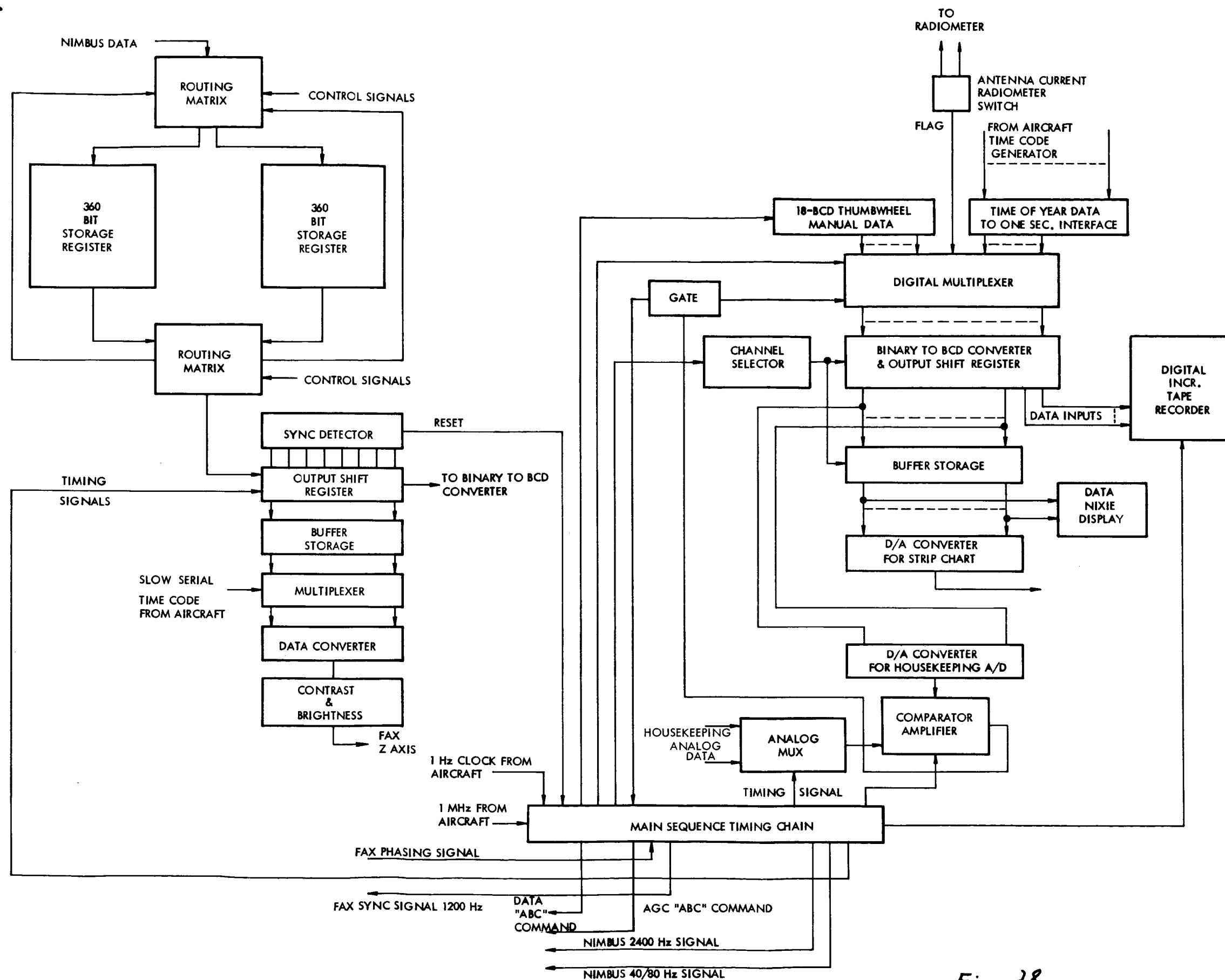


Fig. 28

Figure 28. Scan Converter, Data Acquisition System

Section 3

NIMBUS RADIOMETER TEST SET

The radiometer test set provides interface signals necessary to simulate the NIMBUS spacecraft from the antenna port input to the various telemeter outputs. The test set is capable of calibrating and thoroughly testing all functions of the radiometer. The test set consists of a microwave signal source and telemetry interface circuitry. Figure 29 is a functional block diagram of the test set with the microwave source to the left of the radiometer and the telemetry interface circuitry to the right.

3.1 MICROWAVE SOURCE

For details of the microwave source, see Appendix XXX.

3.2 TELEMETRY INTERFACE CIRCUITRY

The telemetry interfase signals consist of the following four categories:

- a. Analog Signals - The analog signals provide the radiometer readout of reference load temperature, antenna sink temperature, temperature of the hottest point in the module and the radiometer supply voltage.
- b. Digital "A" Signals - The digital "A" signals provide the radiometer readout of the analog to digital converter and the stepped AGC counter state.
- c. Digital "B" Signals - The digital "B" signals provide the radiometer readout of the state of the power, antenna current readout, and fail-safe mode command relays.
- d. Command Signals - The command signals are magnetic latching relay drive pulses which set the state of the power, antenna current readout and fail-safe mode command relays.

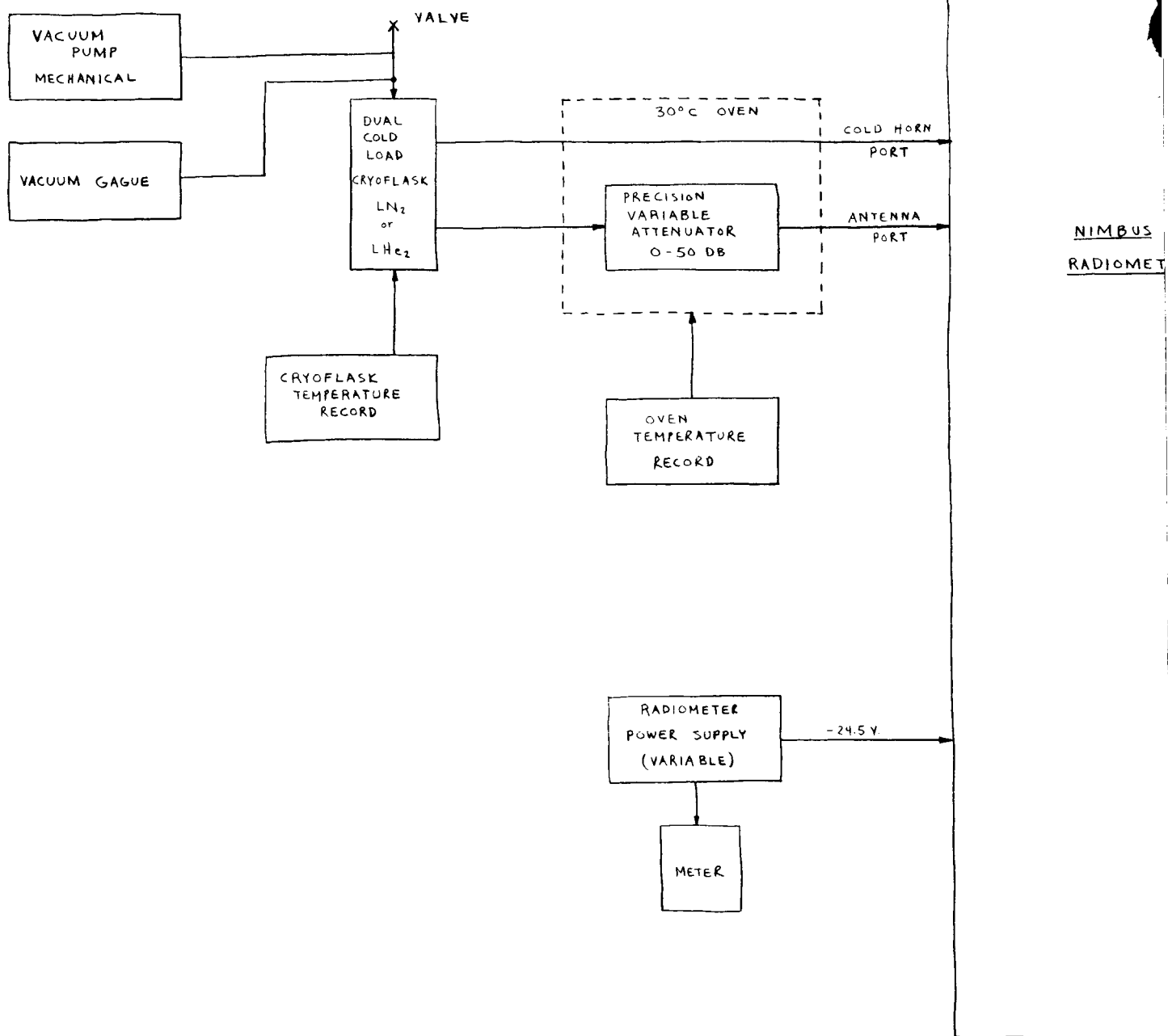
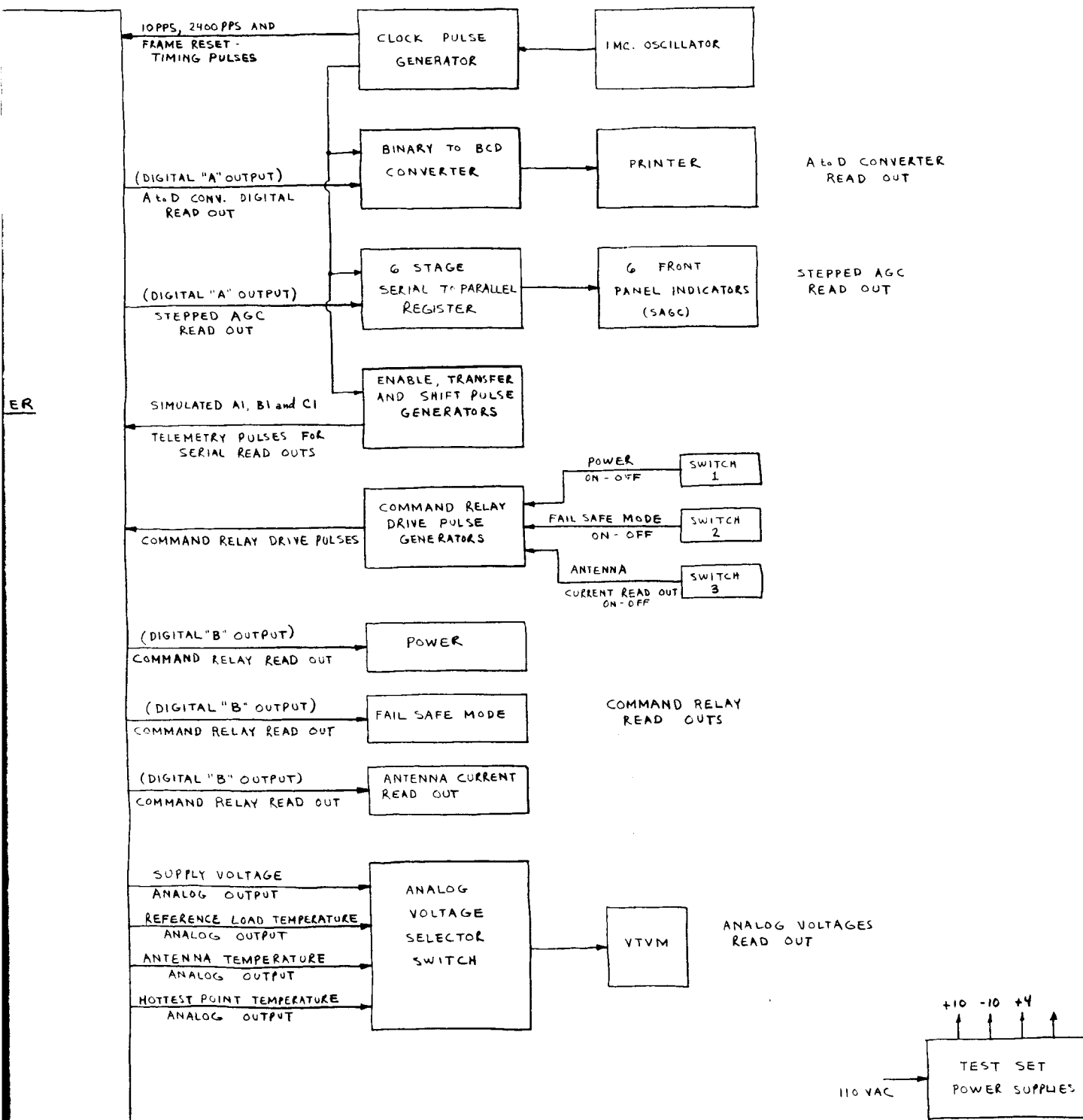


Figure 29. Block Diagram of NIMBUS Ra

45-A



Radiometer Test Set

The information read out from the radiometer is displayed by means of a vacuum tube voltmeter, page printer, and by front panel indicator lamps. The analog outputs are switch selectable and displayed on a 1%, mirrored, vacuum tube voltmeter. The analog-to-digital converter digital "A" output is displayed in decimal format on a page printer. Every 200 milliseconds the count of the analog-to-digital converter is printed as three decimal digits to the right of the printer page, and the parity bit as a one or zero to the left. The stepped AGC digital "A" output is displayed by means of three front panel lamps. The lamps are physically located in the pushbutton switches that generate the command pulses which set or re-set the relays. The supply voltage to the radiometer is indicated by means of an output voltmeter located on the power supply front panel.

In addition to accepting and displaying the above readout signals the test set provides clock and telemetry timing signals to synchronize the radiometer operations and output format to that of the test set. These signals are indicated as 10pps, 2400 pps, frame reset timing pulses, A1, B1 and C1 telemetry pulses in the block diagram. The separate 24.5 volt supply to the radiometer allows the radiometer to be tested throughout its specified supply voltage range.

The timing of all signals and functions generated in the test set is derived from a one megacycle crystal oscillator. Through counters and various logic functions shown in Figure 30 the 1 MHz source is logically manipulated to generate clock rates of 2400 pps, 10 pps, 1 pulse/16 sec. and telemetry reference signals "A1", "B1" and "C1". These signals may be observed at test points TP-6, TP-7, TP-11, TP-8, TP-9 and TP-10 respectively. The format and amplitude characteristics of the telemetry digital "A" interface signals "A1", "B1" and "C1" is shown in Figure 31. The amplitude, rise times and impedance characteristics of the clock signals are identical to the "A1", "B1" and "C1" signal characteristics of Figure 31.

Clock pulses and telemetry pulses provide synchronization timing to the radiometer such that the digital "A" outputs may be read out synchronous to the test set timing. The digital "A" outputs are read into serial to

NOTES:

CARDS 21 - 314 { +5V PIN 2
GND PIN A

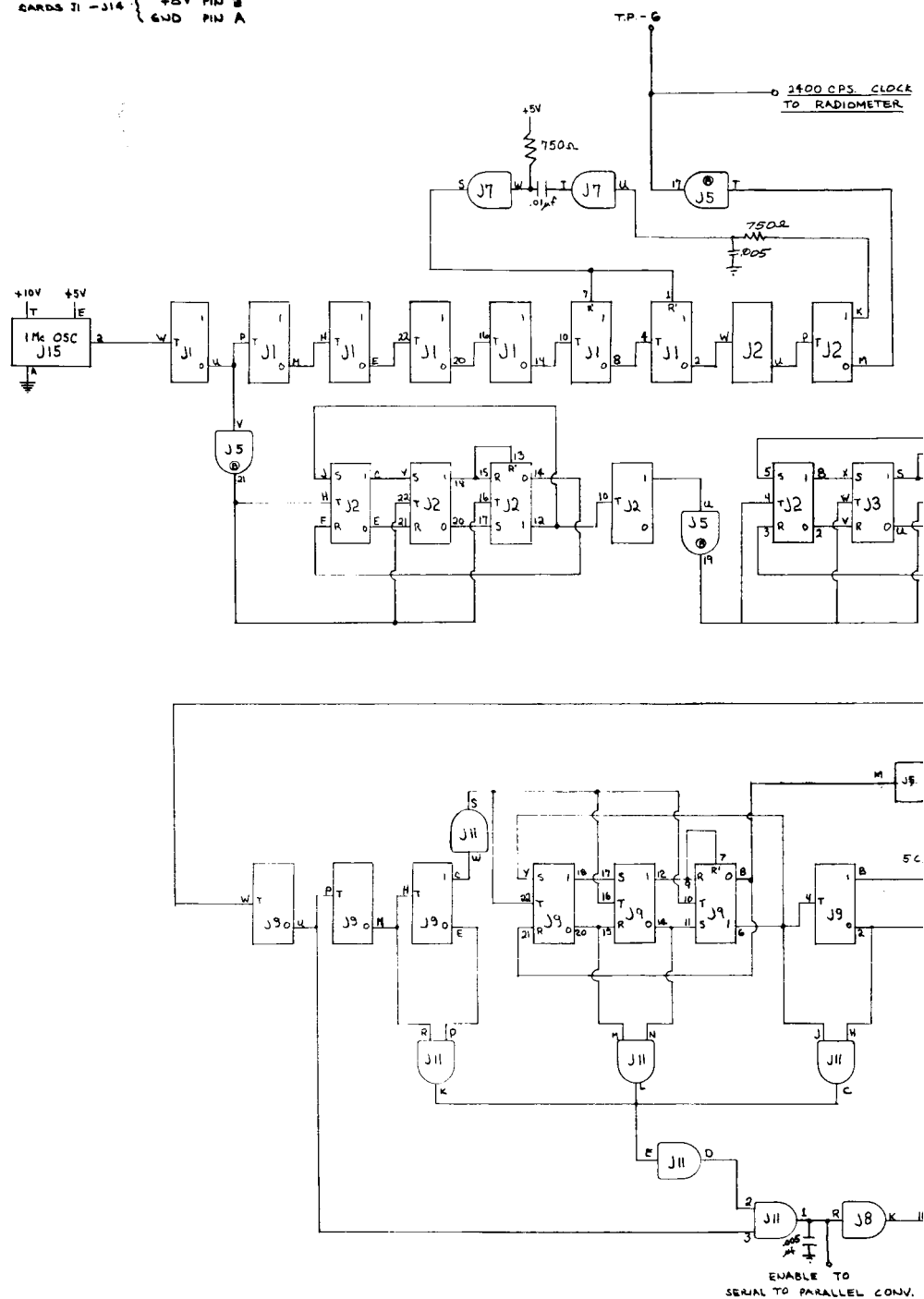
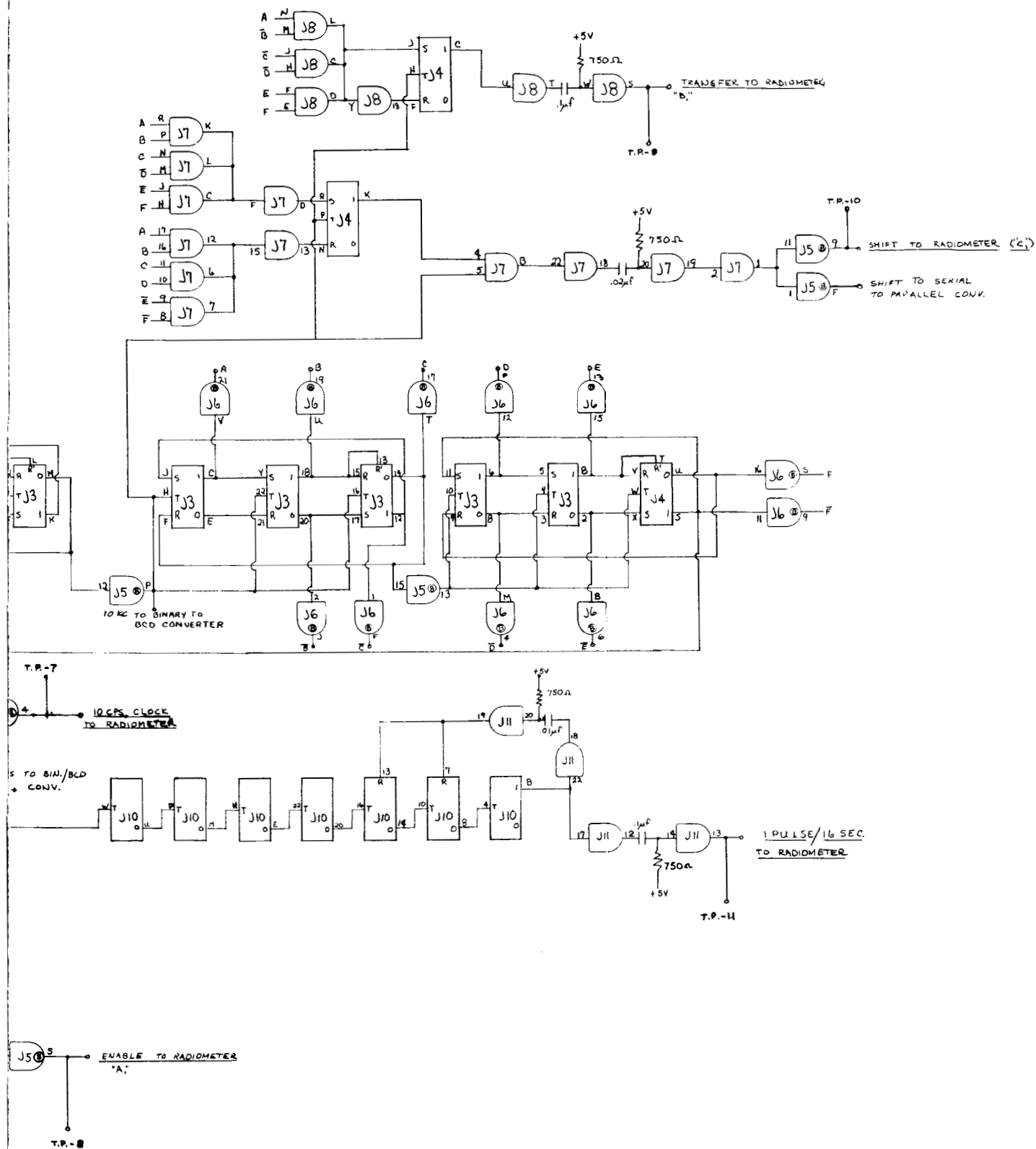
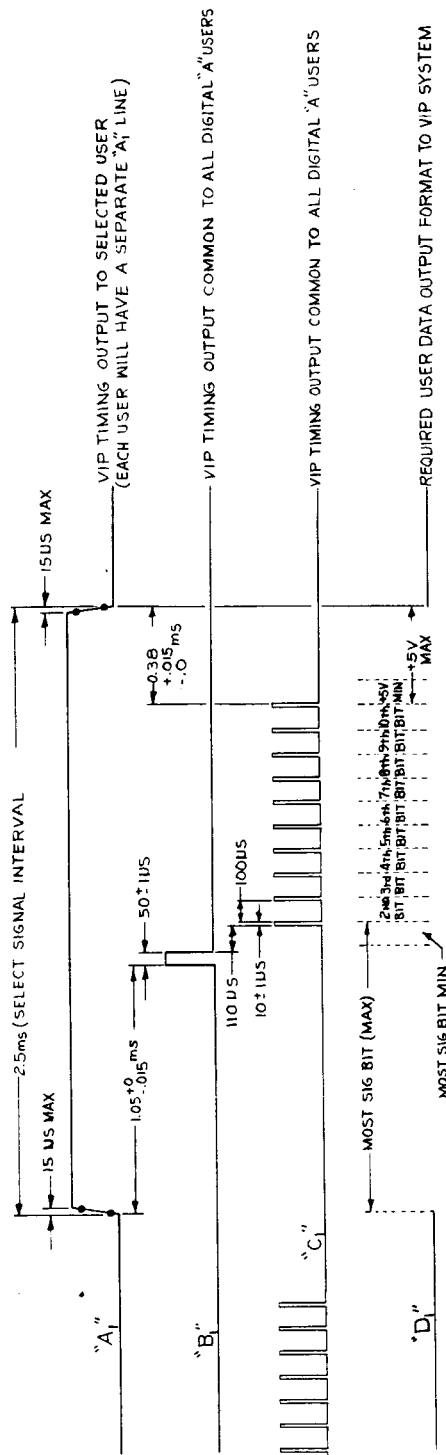


Figure 30. NIMBUS Radiometer Test

47-A



st Set "B", Rack Number 2



REQUIRED OUTPUT CHARACTERISTICS

- 'A': AMPLITUDE 0 ± 0.6 VOLTS OR ± 0.6 VOLTS, $Z_0 = 5,000$ OHMS OR LESS
- 'B': AMPLITUDE 0 ± 0.6 VOLTS OR ± 0.6 VOLTS, $Z_0 = 600$ OHMS OR LESS, RISE & FALL TIME LESS THAN 1 μs
[USER LOAD IMPEDANCE: 20,000 OHMS MIN.; CAPACITIVE LOAD 25 pF MAX.; TRANSFORMER COUPLING RECOMMENDED]
- 'C': AMPLITUDE 0 ± 0.6 VOLTS OR ± 0.6 VOLTS, $Z_0 = 600$ OHMS OR LESS, RISE & FALL TIME LESS THAN 1 μs
[USER LOAD IMPEDANCE: 20,000 OHMS MIN.; CAPACITIVE LOAD 25 pF MAX.; TRANSFORMER COUPLING RECOMMENDED]
- 'D': AMPLITUDE 0 ± 0.6 VOLTS FOR LOGICAL '0' AND ± 0.6 VOLTS FOR LOGICAL '1', RISE & FALL TIME LESS THAN 1 μs WITH EXPERIMENT POWER ON OR OFF, USERS 'D', LOAD IMPEDANCE SHALL BE 1000 OHMS OR LESS

Figure 31. NIMBUS 'D' VIP Digital 'A' Interface

parallel registers in the test set for data processing and display. The analog to digital converter output is read into the serial to parallel converter of the binary to BCD converter shown in Figure 32. The converter output signal from the radiometer will have a "one" level of $+5 \pm 0.6$ volts and a zero level of $0 \pm 0.6V$, an output impedance of 1000 ohms or less and rise and fall times of 1 microsecond or less.

The binary to binary coded decimal converter (Figure 32) is necessary to convert the serial binary output of the A to D converter to BCD form such that the converter count may be displayed decimally and easily interpreted without the use of binary conversion tables. The converter accepts 9-bit parallel data from the serial to parallel input register and converts it, most significant bit first, to binary coded decimal data. The BCD data is stored in a parallel 12-bit 3-decade output register shown at the top of Figure 32. The conversion method used is the double dabble method.

The properties of binary numbers are such that a number may be doubled or halved simply by shifting the number one digit to the right or left with respect to a reference weighting position. A BCD number has the same property, but numbers which have been doubled must be adjusted because a radix of ten has been imposed. Doubling any four-bit number greater than four in quantity results in a number 10 or greater which is beyond the limit of the constraint placed on a decimal digit. By adding six to any number greater than 9, as a result of doubling, a two-digit number is created within a constrained radix of ten.

A convenient method of implementing the "add 6 correction" is to detect 4 bit digits that are greater than four in quantity and add three before doubling. This is equivalent to adding 6 after doubling but results in less hardware by eliminating the need for carry generation between decades.

The method used entails successive doubling, adding and correcting. The quantity in the BCD register is doubled by shifting the BCD number one place to the right and the next binary bit to be shifted into a particular decade is accumulated to the doubled number in that decade. Between each

CARDS 11-115 +4V PIN 8
 CARD 116 +7.5V PIN 8
 ALL CARDS END PIN A

NOTES:

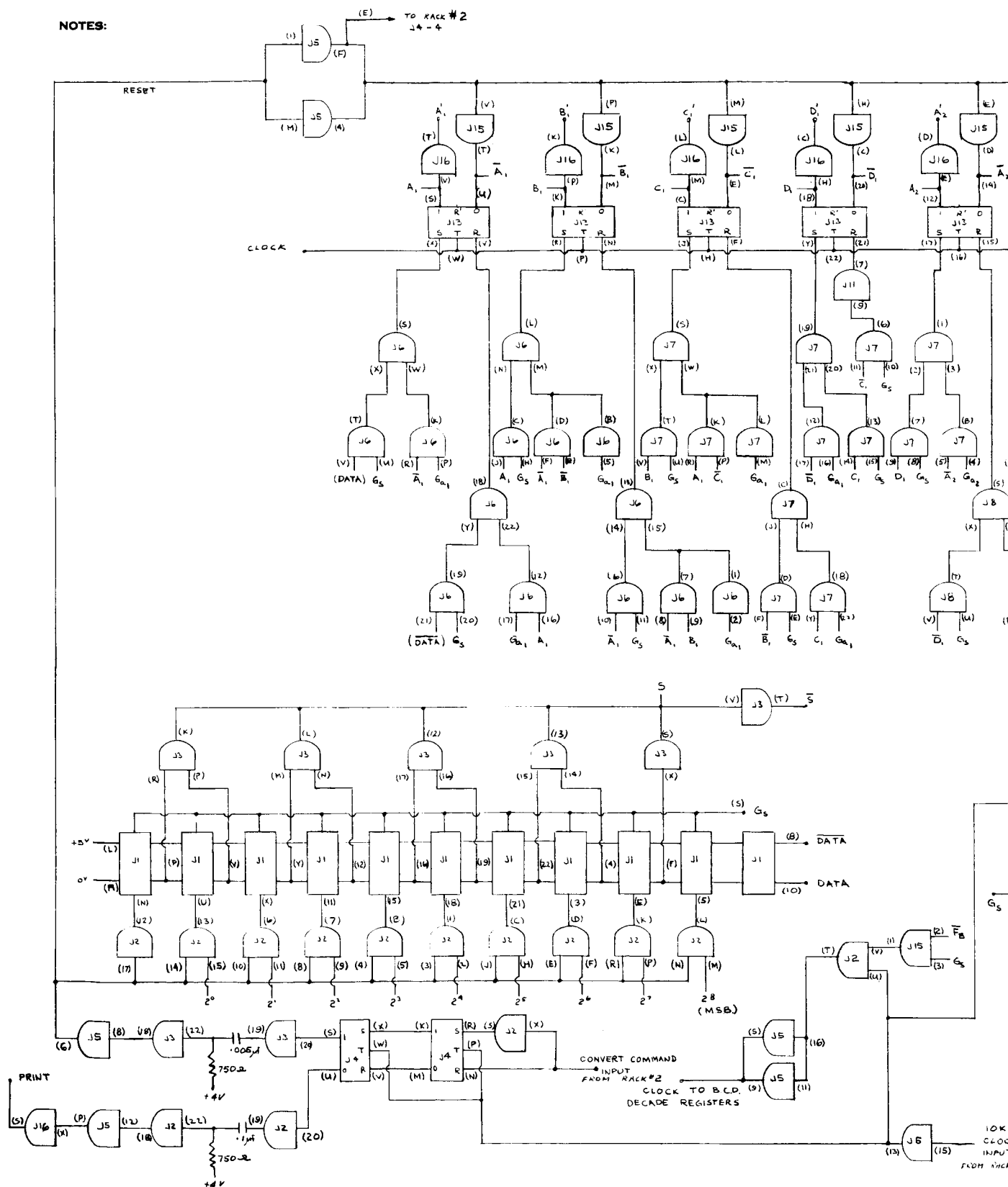
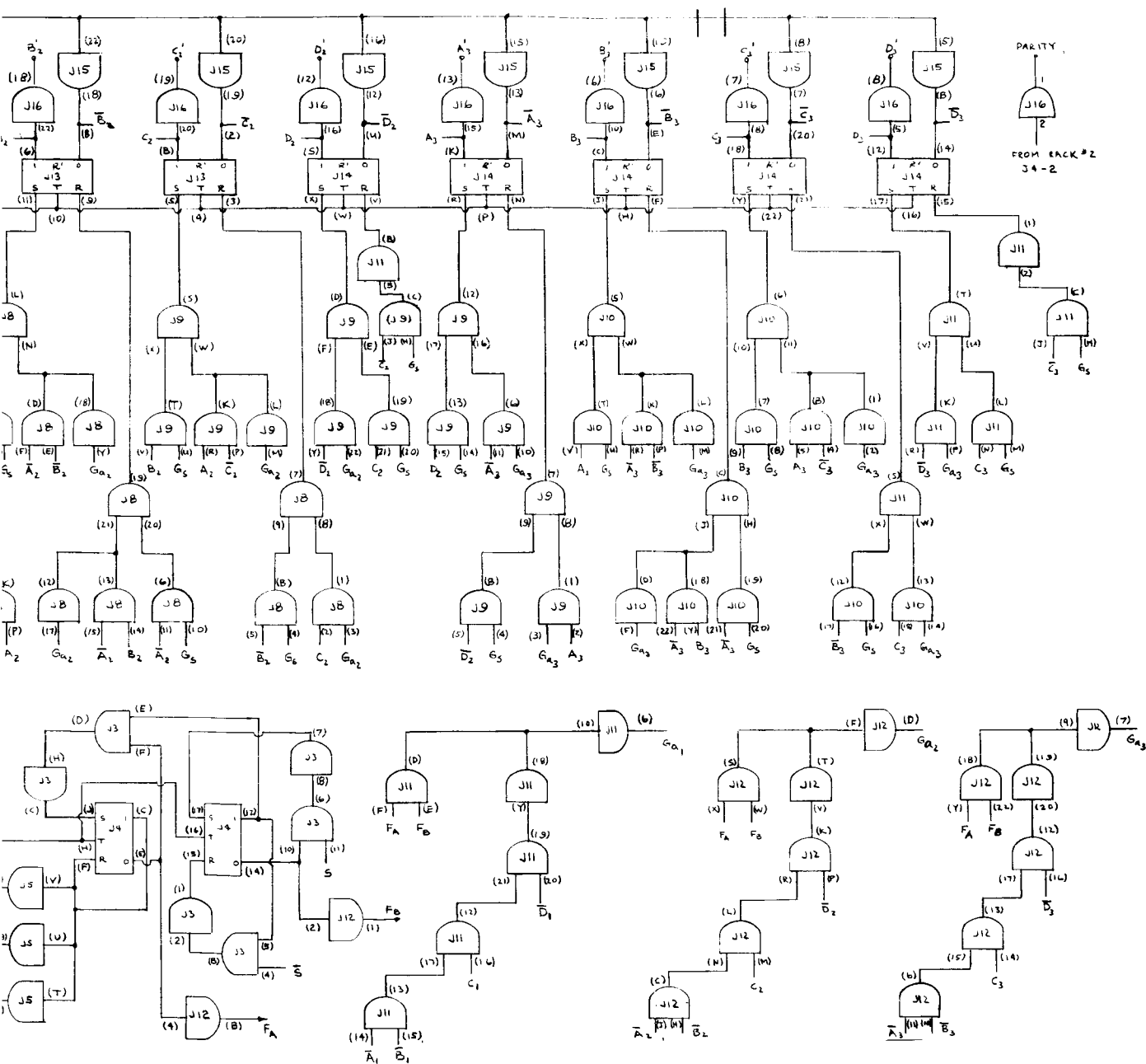


Figure 32. NIMBUS Radiometer Test Set
 Rack 1

50-A



'A' Binary-to-BCD Converter,

shift and add cycle the size of the number in each decade register is examined. If the number is greater than 4, an add cycle occurs, adding 3 and thereby generating the necessary correction factor. Each of the three decades are identical. The control logic and shift gate are shared by all decades but a separate add gate is mechanized for each decade. The BCD three decade output register feeds the BCD printer input through gates which act as buffer amplifiers to increase the output logic voltage level. A delayed conversion command is used as the print command to the page printer.

The frame format read out of the radiometer in the normal operating mode was shown in Figure 4. The frame reference (noted as frame identification, frame time increment Number 480 in Figure 4) prints out all zeros indicating that the next print out or time period is the beginning of a new frame (period number 1). The frame consists of twelve subframes each in turn consisting of 40 frame time periods corresponding to 40 decimal print outs. The first 39 frame periods are a readout of the temperature differential between the hot load and the antenna times the radiometer gain factor for the 39 antenna beam positions respectively. The 40th period of every odd subframe is a readout of the temperature differential between the hot load and cold horn references times the radiometer gain factor. Since the temperatures of the hot and cold references are known the radiometer gain factor and ultimately the radiometric temperatures seen by the antenna for each beam position may be calculated. The 40th time period of every even subframe is a readout of various parameters time multiplexed into the frame such as antenna sink temperature, hot load temperature, etc. The frame time increments are 200 ms in duration, therefore, the printer reads out at 5 lines per second.

The second mode of radiometer operation is a housekeeping mode in which the current levels corresponding to each of the 39 beam positions of all 49 antenna coils are serially read out. This mode of operations is initiated by setting the "antenna current readout" command relay. In this mode the A to D converter quantizes input voltage levels which correspond to the various current levels of the antenna coils and the print out, therefore,

is an indication of the beam steering computer operation since the beam steering computer supplies the antenna beam positioning currents. This read out is not meant to be a precise absolute current display but a relative indication of the 1911 current levels with respect to each other such that any gross error in a particular current level such as zero current or saturating current caused by a catastrophic component failure will be observed.

The frame format of the antenna current readout is shown in Figure 6 of Appendix XXIII. As in the normal mode format the frame consists of subframes each 40 frame periods in length. In the antenna current readout mode, however, a total frame consists of 50 subframes. The first 49 subframes readout 39 coil current levels corresponding to 39 beam positions and zero current during the 40th time period for the 49 antenna coils. The 50th subframe reads out full scale (saturation) for the purpose of frame identification. Four hundred seconds is required to readout an entire frame since the frame time period again is 200 microseconds.

The serial stepped AGC output is synchronously read into the serial to parallel display register shown in the upper left hand corner of Figure 33. The input signal amplitude, rise time and impedance is identical to that of the A to D converter output signal. Although the word read in is ten bits in length, only the first six bits are significant information. The last six stages, therefore, of the register feed lamp drivers and front panel lamps which indicate the states of the six flip flops of the stepped AGC counter in the radiometer. The lamps indicate the attenuation of the stepped AGC circuit in binary weighted increments, 1/2 dB, 1 dB, 2 dB, 4 dB, 8 dB, and 16 dB respectively.

The command relay pushbutton switches, one shots, and relay driving circuits are shown in the upper right hand corner of Figure 33. Each time a pushbutton is depressed the corresponding flip flop toggles. Each toggle alternately fires the right then left hand one shot which in turn generates pulses alternately to the set and reset coils of the corresponding command relay. Therefore, each time a given pushbutton switch is depressed the corresponding command relay in the radiometer changes states from open to closed and vice versa.

CARDS J1-J14, J19 — +5V PIN 2
 CARDS J16 & J17 — { +10V PIN 1
 - 24.8V PIN 2
 ALL CARDS — GND PIN A

NOTES:
 LAMPS &
 SWITCHES
 MOUNTED ON
 FRONT PANEL

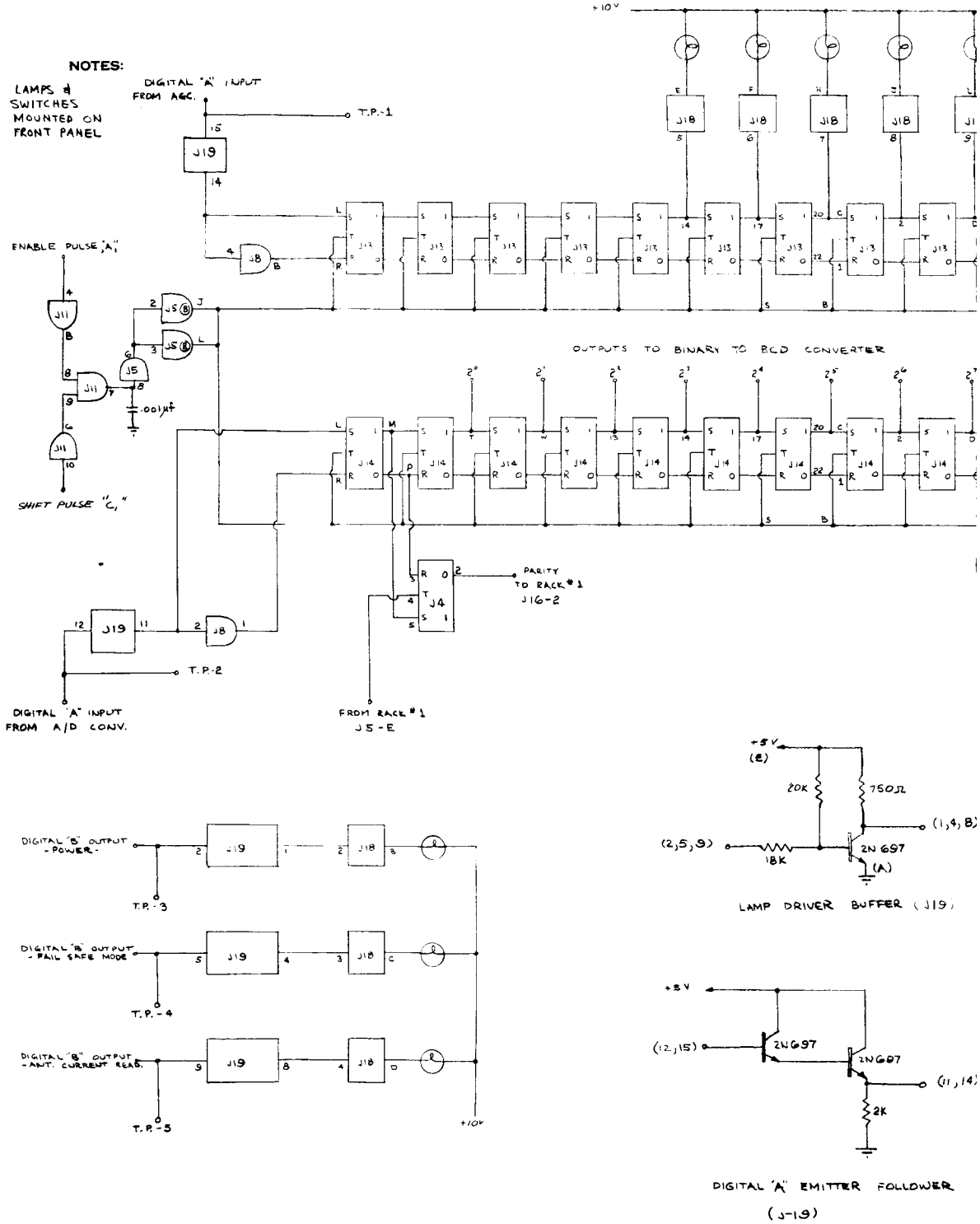
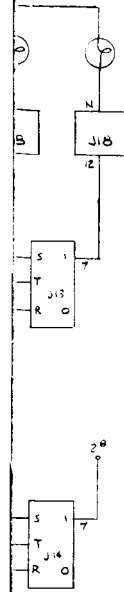
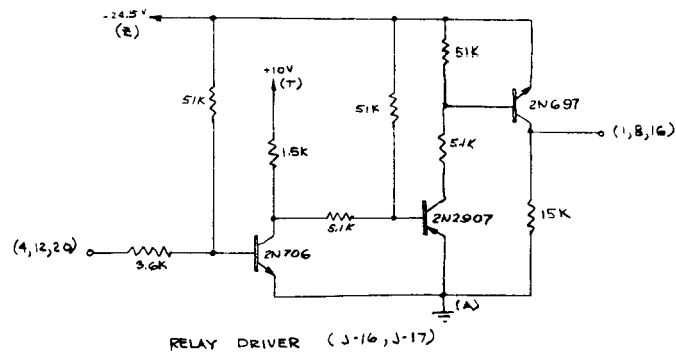
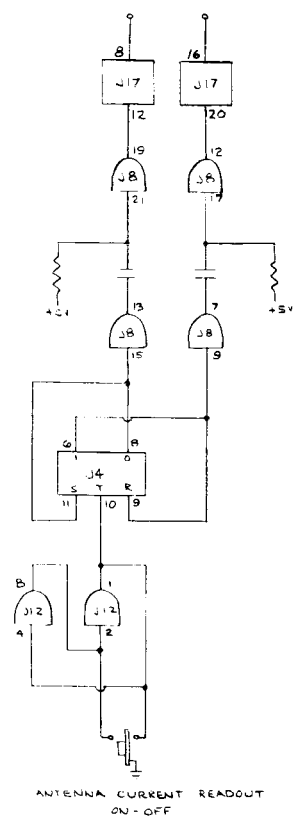
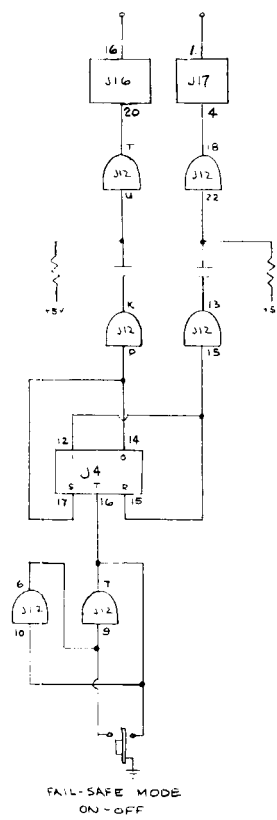
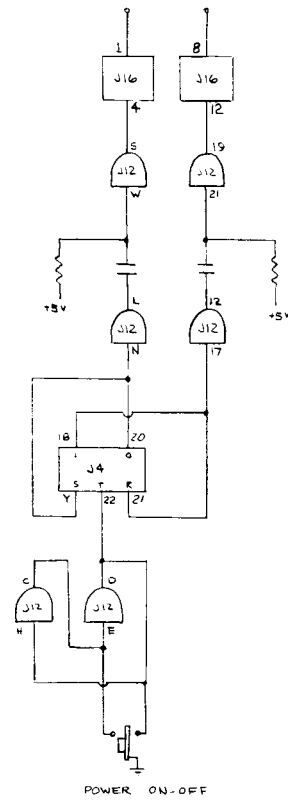


Figure 33. NIMBUS Radiometer

53-A



PULSES TO COMMAND RELAYS



The state of the command relays is indicated by the digital "B" outputs (0 to 7.5 volts) which feed the emitter follower-lamp driver circuits in the lower left hand corner of Figure 33. The lamps are physically located in the pushbutton switches and light when the function they describe is operative.

Figure 34 is a detailed connector interface schematic showing all interface signals and wires between the radiometer and the test set.

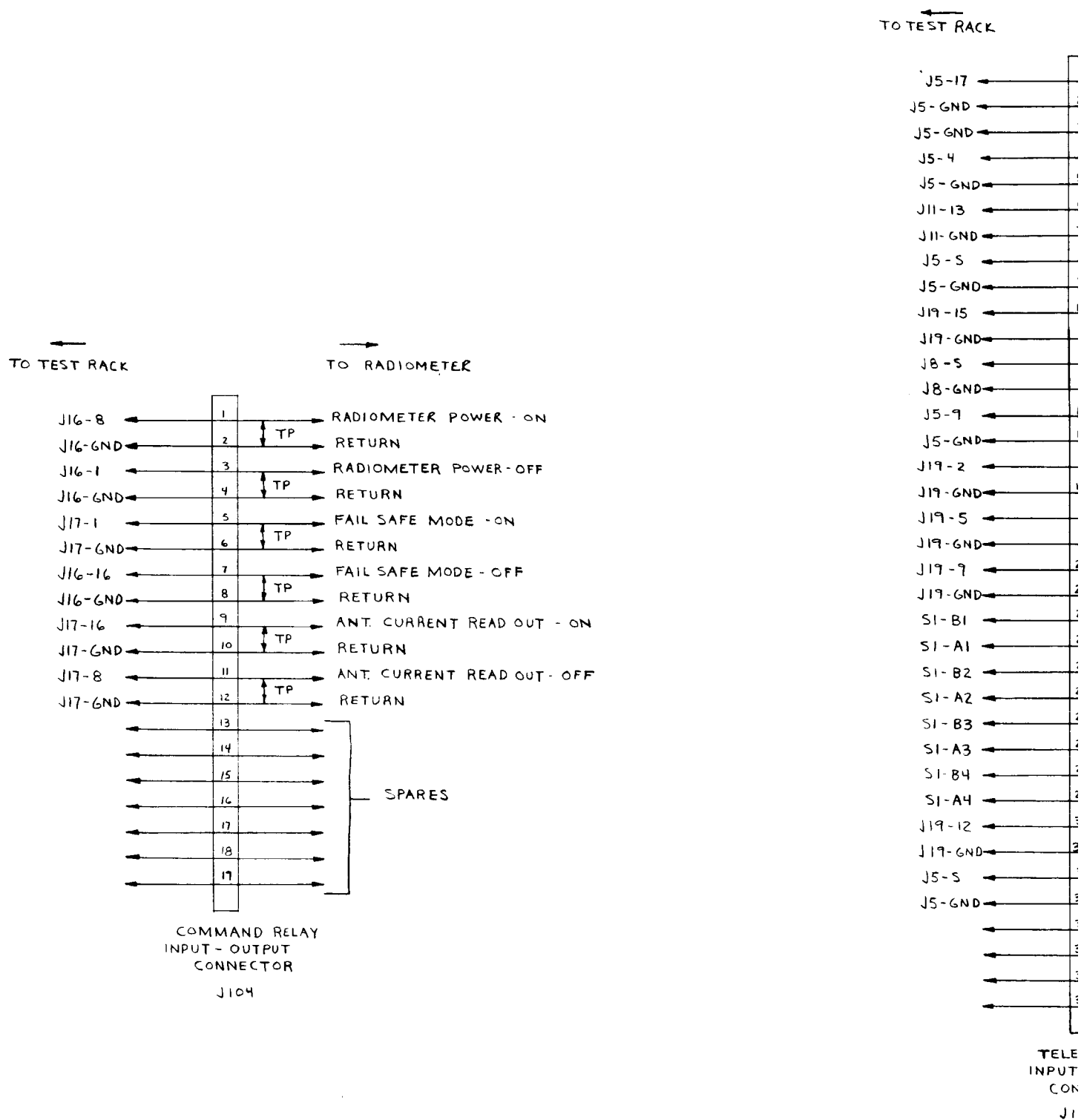
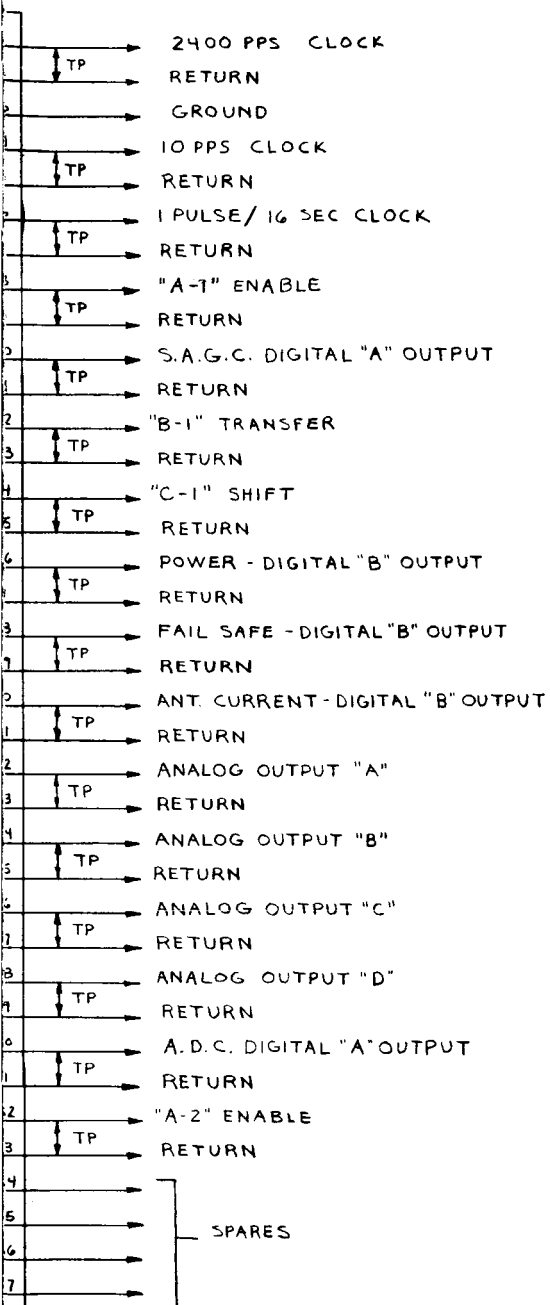


Figure 34. NIMBUS Radiometer Test Set

55-A

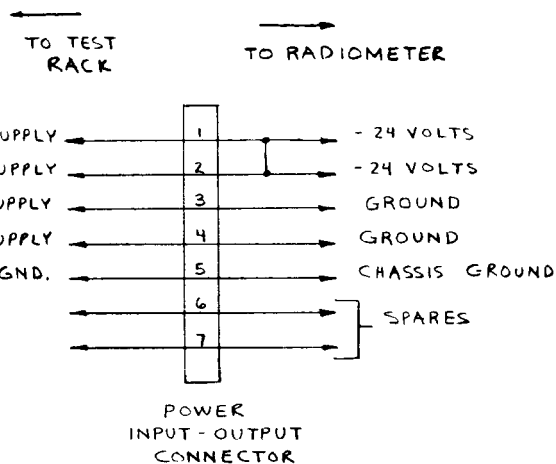
TO RADIOMETER



METRY
- OUTPUT
NECTOR

53

Input-Output Connectors



Section 4

DATA ACQUISITION AND DISPLAY SYSTEM

The meteorological radiometric data acquisition and display system is a device which commands, times, and records the operation of the meteorological radiometer while providing a time history gray scale representation of the scanned radiometric output values.

The gray scale display of the radiometric output values are arranged with each antenna scan position displayed sequentially across the width of the display paper. The display is corrected in the cross-track dimension for scan intercept and antenna distortions. The continuous gray scale history is provided by using a commercially available facsimile printer as the display device. Continuously variable bias and amplitude controls are provided to allow for the detailed examination of a portion of the radiometric output values within the resolution capability of the human eye.

Concurrently with the gray scale display of the radiometric values, all information generated within the radiometer, as well as separately gathered support information, is recorded on a computer compatible digital magnetic tape.

As a diagnostic aid, any portion of the data as it is recorded on a digital magnetic tape, may be displayed in a decimal manner on a digital display. Selection of the required portion of the data for display is implemented by a combination of thumb wheel and rotary switches. The data segment selected by these switches is also available, at the same time, in a continuous analog form, for use on a strip chart recorder.

The data acquisition and display system is designed to operate in an exact-time synchronous manner with other similar types of systems operating at the same time. In order to facilitate time-synchronous operation, the system has no local frequency source or time accumulating section and therefore, requires these signals and information to be supplied to it from

external sources for operation. In addition to the normal supply power requirements, a one MHz signal is required for the system. To phase the system operation with other external equipment, a one pulse per second signal must be applied and this signal must be in phase with the 1 MHz frequency. The system will record, on the digital magnetic tape, time information including day of the year, hour of the day, minute and second if it is supplied to the system in a parallel manner in the appropriate code and at the appropriate location.

Time correlation capability for the facsimile display is provided by the recording, on the facsimile paper of a black and white representation of a serial time code supplied to the system from an external source.

To allow a degree of flexibility in data gathering, the system will function as the meteorological radiometer at two different data integration rates.

With all of the appropriate connections made to the system, the system functions in the following manner: The 1.0 MHz externally supplied clock signal is counted down within the system to produce the 2400 Hz signal required by the meteorological staellite. Depending upon which of the two radiometer integration times is being used, the 2400 Hz signal is further counted to either 80 or 40 Hz. This frequency is used to control the integration time of the radiometer. The 80 or 40 Hz signal is counted down by a factor of 80, which in turn produces a frequency of 1 or 0.5 Hz. This frequency is used to reset the subframe counter within the radiometer and maintains the data acquisition system and the radiometer in synchronization. The 1 or 0.5 Hz signal is further counted down by a factor of twelve to produce a reset signal to phase the data acquisition system and the radiometer subframe counters. Additional signals are derived from the data acquisition count-down chain to produce the A, B, and C commands required to read the digitized radiometric values from the radiometer. As each value is received from the radiometer, the associated parity bit is removed and the remaining nine bits of data are inserted into a 360-bit serial-storage register. This 360-bit storage register is large enough to accept all of the data obtained from one complete scan of the radiometer. After one complete scan

is received in the 360-bit storage register, the data associated with the next subframe is routed to a second identical 360 storage register. The data contained within the first 360-bit register is read out and recycled back into the register one nine-bit word at a time. As each nine-bit word is read out the resulting value is transferred to a holding register and the output of the holding register is converted to an equivalent analog voltage. This analog voltage is used to modulate the writing edge of the facsimile display unit and produce the gray scale representation of the radiometric data. The readout rate of the 360-bit register is controlled by a separate local oscillator whose frequency may be varied by means of a front panel control on the data acquisition system. Varying the frequency of this local oscillator increases or decreases the width presentation of a given radiometric scan line on the facsimile display. The readout rate of each scan position of a given scan line is varied to present the data on the facsimile recorder in the same proportion as the antenna beam intercepts the ground. The facsimile display unit produces a line approximately one hundredth of an inch wide for each input. In order to provide a display with a reasonably large dimension, the data contained within the 360-bit register is recycled and redisplayed on the facsimile display unit four times for the fastest integration time and eight times for the slower integration time. The beam dimension at the center of the scan is assumed to be the same in both horizontal and vertical dimension so the presentation on the facsimile display for a center beam position is approximately four tenths of an inch by four tenths, for the fastest integration time, and approximately eight tenths of an inch by eight tenths of an inch for the slower integration time, with the local readout oscillator operating at the center of its range. Just prior to the time that a given scan line is to be read out of the 360-bit storage register for display, a standard number is fed to the digital-to-analog converter used to modulate the facsimile display system. This standard number varies in precise steps with each scan line of the radiometer and the series of numbers repeats with each major frame of the radiometer. This series of standard numbers encompasses the range of values obtained from the radiometric system and provides a standardized display of intensities that are used to determine over what range of the radiometric data the facsimile unit

is operating. After the forty radiometric data values have been displayed (39 radiometric output values, plus one channel of subcommutator data), an externally supplied signal representing a serial time code is applied directly, to modulate the facsimile writing edge. One complete scan of the facsimile display takes 250 milliseconds. Providing a picture with the correct aspect ratio at the slowest integration time leaves 40% of this time when the radiometric data are not modulating the facsimile unit. During this time interval the data in the storage register are again recycled and read out, but this time the data are applied to the digital tape record. There is not sufficient time available when data are not presented as the facsimile unit, during one scan, to read all of the available data to the tape recorder. At the highest integration time, the data is recycled four times for displays. The data readout to the tape is separated into four groups for recording on the tape recorder. The data within the 360-bit register are then recycled a total of 8 times, 4 times for the display, and 4 times for digital recording, when operating at the highest integration time. After completion of another reading of a scan line from the radiometer, the above described operation has been completed and the action of the two 360-bit shift registers is toggled and the operation is repeated.

During the time interval that the radiometric data is being presented to the facsimile display other support information such as the radiometer AGC step, externally supplied parallel time code, and the internal analog to digital converter output, are recorded on the digital magnetic tape.

As a diagnostic aid, logic circuits and switches are provided for the selection and display of any of the radiometric data and the internal analog to digital converter data on decimal indicators. The data which are provided in binary form are first converted to binary coded decimal before display. Any data value selected for display is also available at the same time converted to an equivalent analog voltage.

The tape recorder automatically inserts a $3/4$ " tape gap after the completion of the recording of a full major frame of output of the radiometer data. This procedure simplifies later computer processing. When a digital data record is terminated, the tape recorder records until the next full major frame of radiometric data has been completed. At this point the data are no longer recorded, the tape recorder advances $3-1/2$ inches of tape writes an end of file mark and advances an additional $3/4$ inch and stops. This procedure provides a discrete indication to the computer of end of a given record.

Section 5

CALIBRATION PROCEDURE SUMMARY

To calibrate the NIMBUS radiometer and antenna (for measuring brightness temperatures to within 2 degrees Kelvin) two sets of procedures are required. One set is for bench test calibration of the radiometer and the other is for the field test calibration of the antenna.

A dual microwave port cryoflask is used as a cold load. Connected to one port is a precisely calibrated section of waveguide. This connects to the cold reference port of the radiometer and is used to establish the cold end of the transfer characteristic and AGC reference. Connected to the other port is a precision attenuator. This, in turn, connects to the antenna port of the radiometer.

The cryoflask is cooled using liquid nitrogen at the boiling point of nitrogen and establishes a cold reference point. It also establishes the cold end of the radiometer transfer characteristic when the attenuator is set at zero (zero attenuation). By increasing the attenuation, the radiometric temperature is raised to the kinetic temperature of the attenuator. Thus, by starting at zero attenuator setting and increasing the attenuation, a transfer characteristic can be generated for the radiometer. The temperature at the antenna port of the cryogenic cold load is given by the following expression:

$$T_{eq} = T_{\frac{L}{L}} + \left[1 - \frac{1}{L} \right] T_{AMB}$$

where

T_{eq} = Equivalent brightness temperature in °K

L = Loss (power ratio)

T_{AMB} = Ambient temperature in °K

T_L = Cryogenic boiling point in °K

In this case the loss is due solely to the attenuator. Maximum attenuation results in T_{AMB} as shown by the above expression. For a detailed explanation of the cold load test set refer to the Calibration Handbook.

Since an antenna is connected to the radiometer in place of the cryogenic test set, in actual use, any temperatures seen at the antenna port of the radiometer are a result of radiation from the antenna plus the atmosphere and target. If the antenna is calibrated then using the transfer characteristic generated by the cryogenic test set the temperatures read by the radiometer can be referred to the antenna aperture. To refer the temperature from the radiometer antenna port to the antenna aperture the following expression is used:

$$T_R = \frac{E}{L_a} P_{im} + P_{is} \frac{(1 - E)}{L_a} + \frac{(L_a - 1)}{L_a} t$$

where

T_R = radiometer output temperature in $^{\circ}K$

E = antenna main beam efficiency

L_a = antenna dissipative loss

P_{im} = power incident from main beam in watts

P_{is} = total incident power from side lobes in watts

t = antenna kinetic temperature in $^{\circ}K$

In this expression it can be seen that the antenna losses (L_a) and beam efficiency (E) must be known. To calibrate the antenna these losses are measured by locating the equipment on a mountain or some high altitude platform where the effects of the atmospheric water vapor are removed or minimized. The antenna is directed towards zenith and all side lobes are directed upward by reflecting plates.

In this case the equation then becomes

$$T_R = \frac{P_{im}}{L_a} + \frac{(L_a - 1)}{L_a} t$$

By enclosing the antenna in an insulated box which is radiometrically transparent the antenna temperature is raised. Also the sky temperature at zenith is quite cold. Thus P_{im}/L_a becomes small and the equation becomes

$$T_R = \left(\frac{L_a - 1}{L_a} \right) t$$

L_a is then calculated from knowing T_R and t .

To achieve this beam efficiency calibration, an absorbing disc is placed in the main beam sufficiently large to encompass the main beam at the nulls. The kinetic temperature of the disc is measured. The side lobes are directed toward the sky, however, no side lobe energy should be directed toward the absorbing disc. Using the expression

$$T_R = \frac{P_{im} E}{L_a} + \frac{P_{is}}{L_a} (1 - E) + \frac{(L_a - 1)}{L_a} t$$

T_R is known, L_a is known, t is known, and P_{im} is known since

$$P_{im} = K \beta T$$

where

K = Boltzman's constant

β = bandwidth of the radiometer

T = kinetic temperature of the disc

P_{is} is extremely small because the sky temperature is quite cold (approximately 3.5°K).

Therefore the expression can be reduced to

$$T_R \approx \frac{P_{im} E}{L_a} + \frac{(L_a - 1)}{L_a} t$$

E then can be calculated.

Now the antenna has been calibrated. Using the transfer characteristic, T_R is then established in terms of temperature, and P_{im} can be calculated. For

a more detailed explanation of this calculation refer to the Calibration Handbook. All kinetic temperature measurements and all insertion loss measurements were 10 to 100 times more accurate than the accuracy of the radiometer. Temperatures were measured using thermistors calibrated at the National Bureau of Standards. Insertion loss measurements of the waveguide were performed with a precision insertion loss bench test set. This set was calibrated by the Space-General Calibration Laboratory.

Boiling point temperatures were corrected for pressure in accordance with the National Bureau of Standards pressure of vaporization standards. Atmospheric watervapor content was monitored continuously and checked with JPL test site measurements. Air temperature was monitored continuously and checked with JPL test site measurements.

All tests were performed several times in order to give a statistical average, thereby avoiding best or worst case measurements.

The techniques used in the calibration of the antenna and radiometer proved to be adequate to calibrate to within 2°K absolute. Tests proved these techniques to be sufficient for higher accuracy, however, refinements would be required to measure all parameters with a higher degree of precision.